© 2022. Published by The Company of Biologists Ltd | Development (2022) 149, dev200560. doi:10.1242/dev.200560

RESEARCH ARTICLE

Plexin D1 negatively regulates zebrafish lymphatic development

Denver D. Britto[1], Jia He[2], June P. Misa[1], Wenxuan Chen[1], Purvi M. Kakadia[1,3], Lin Grimm[4,5,6], Caitlin D. Herbert[1], Kathryn E. Crosier[1], Philip S. Crosier[1], Stefan K. Bohlander[1,3], Benjamin M. Hogan[4,5,6], Christopher J. Hall[1], Jesús Torres-Vázquez[2] and Jonathan W. Astin[1,*]

ABSTRACT

Lymphangiogenesis is a dynamic process that involves the directed migration of lymphatic endothelial cells (LECs) to form lymphatic vessels. The molecular mechanisms that underpin lymphatic vessel patterning are not fully elucidated and, to date, no global regulator of lymphatic vessel guidance is known. In this study, we identify the transmembrane cell signalling receptor Plexin D1 (Plxnd1) as a negative regulator of both lymphatic vessel guidance and lymphangiogenesis in zebrafish. *plxnd1* is expressed in developing lymphatics and is required for the guidance of both the trunk and facial lymphatic networks. Loss of *plxnd1* is associated with misguided intersegmental lymphatic vessel growth and aberrant facial lymphatic branches. Lymphatic guidance in the trunk is mediated, at least in part, by the Plxnd1 ligands, Semaphorin 3AA and Semaphorin 3C. Finally, we show that Plxnd1 normally antagonises Vegfr/Erk signalling to ensure the correct number of facial LECs and that loss of *plxnd1* results in facial lymphatic hyperplasia. As a global negative regulator of lymphatic vessel development, the Sema/Plxnd1 signalling pathway is a potential therapeutic target for treating diseases associated with dysregulated lymphatic growth.

KEY WORDS: Plexin D1, Lymphatic, Zebrafish, Lymphangiogenesis, VEGFR

INTRODUCTION

The lymphatic system is a network of vessels that are essential for interstitial fluid homeostasis with secondary roles in immune cell trafficking and lipid absorption. Dysregulated lymphangiogenesis has been implicated in a number of health conditions that include, lymphoedema (Brouillard et al., 2021; Saito et al., 2013), tumour metastasis (Stacker et al., 2014) and graft rejection (Dashkevich et al., 2016; Dietrich et al., 2010; Ishii et al., 2010; Pedersen et al., 2020; Wong, 2020).

Lymphatic endothelial cells (LECs) are mostly specified in the venous endothelium, via the action of the transcription factor PROX1 (Srinivasan et al., 2007; Wigle et al., 2002; Wigle and Oliver, 1999; Yaniv et al., 2006). The migration and proliferation of LECs is stimulated through VEGFR3 signalling in LECs, where the binding of VEGFC to VEGFR3 stimulates downstream signalling through the AKT/PI3K and MEK/ERK pathways to promote migration, proliferation and survival (Baek et al., 2019; Coso et al., 2012; Deng et al., 2015; Grimm et al., 2019; Hägerling et al., 2013; Hogan et al., 2009b; Karkkainen et al., 2004; Küchler et al., 2006; Salameh et al., 2005; Shin et al., 2016). Although the pathways that drive lymphangiogenesis are relatively well studied, the mechanisms that regulate this process are less well understood.

The ability to image the entire larval lymphatic network, *in vivo*, make zebrafish an ideal model for discovering global regulators of lymphatic vessel growth (Jung et al., 2017; Okuda et al., 2012; Yaniv et al., 2006). In the zebrafish trunk, LECs migrate from the posterior cardinal vein (PCV) at 36 hpf to the horizontal myoseptum to form parachordal LECs (Bussmann et al., 2010; Hogan et al., 2009a; Yaniv et al., 2006). These parachordal LECs then migrate along the arterial intersegmental blood vessels (aISVs) to form the trunk lymphatic network, which by 6 dpf consists of intersegmental lymphatic vessels (ISLVs), the thoracic duct (TD) and the dorsal longitudinal lymphatic vessel (Bussmann et al., 2010; Okuda et al., 2012). In the zebrafish head, facial LECs are specified in the common cardinal vein, primary head sinus and from a non-venous progenitor called the ventral aortal lymphangioblast. By 6 dpf these progenitors have coalesced to form the otolithic lymphatic vessel (OLV), the medial facial lymphatic (MFL) and lateral facial lymphatic (LFL) (Eng et al., 2019; Okuda et al., 2012). Importantly, all of these vessels form in a reproducible pattern with little individual variation, suggesting that the migration and growth of both the trunk and facial lymphatic guidance is tightly regulated. It is known that specific populations of neurons, arterial mural cells and fibroblasts are required for growth of lymphatics in the zebrafish trunk, and that both mature Vegfc and the chemokine ligands Cxcl12a and Cxcl12b are involved in mediating the aISV/LEC interaction in the zebrafish trunk (Cha et al., 2012; Lim et al., 2011; Peng et al., 2022; Wang et al., 2020). However, to date, no global regulator of lymphatic vessel guidance has been identified.

We conducted a forward genetic screen to identify novel regulators of lymphatic development and uncovered a loss-of-function *plexind1* mutant displaying a novel lymphatic misguidance and overgrowth phenotype. PLXND1 is part of a family of large transmembrane cell-signalling receptors that have roles in both axon and vascular guidance (Zhang et al., 2021). PLXND1 is expressed within endothelial cells and is activated primarily by binding to either secreted or membrane-tethered semaphorin (SEMA) ligands, which results in modulation of endothelial cell migration, growth and adhesion. Previous work has shown that PLXND1 has a conserved role in inhibiting the growth of blood vessels through antagonising VEGFR signalling and by regulating actin polymerisation within endothelial cells (Childs et al., 2002; Fukushima et al., 2011; Gitler et al., 2004; Gu et al., 2005;

[1]Department of Molecular Medicine and Pathology, School of Medical Sciences, University of Auckland, Auckland 1023, New Zealand. [2]Skirball Institute of Biomolecular Medicine, New York University Grossman School of Medicine, New York, NY 10016, USA. [3]Leukaemia and Blood Cancer Research Unit, Department of Molecular Medicine and Pathology, Faculty of Medical and Health Sciences, The University of Auckland, Auckland 1023, New Zealand. [4]Organogenesis and Cancer Program, Peter MacCallum Cancer Centre, Melbourne 3000, Australia. [5]Sir Peter MacCallum Department of Oncology, University of Melbourne, Melbourne 3010, Australia. [6]Department of Anatomy and Physiology, University of Melbourne, Melbourne 3010, Australia.

*Author for correspondence (j.astin@auckland.ac.nz)

J.P.M., 0000-0002-4474-4672; L.G., 0000-0001-7807-2096; J.W.A., 0000-0002-3554-0133

Handling Editor: Steve Wilson
Received 24 January 2022; Accepted 23 September 2022

Development (2022) 149, dev200560. doi:10.1242/dev.200560

Kim et al., 2011; Moriya et al., 2010; Tata et al., 2014; Torres-Vázquez et al., 2004; Zhang et al., 2009; Zygmunt et al., 2011). Although the molecular mechanisms that underpin PLXND1-mediated anti-angiogenesis are still not clear, it is thought that upon ligand binding, the GTPase-activating protein (GAP) domain of PLXND1 is activated, leading to the deactivation of Rho-GTPases, resulting in the disruption of integrin-mediated cell adhesion, downregulation of both ERK and MAPK signalling, and modulation of the actin cytoskeleton (Gay et al., 2011; Zhang et al., 2021). In mice, SEMA3C, SEMA3D and SEMA4A have all been implicated in the negative regulation of blood vessel growth through PLXND1 (Gu et al., 2005; Toyofuku et al., 2007; Yang et al., 2015). In zebrafish, Sema3 and Plxnd1 signalling is essential for intersegmental blood vessel (ISV) guidance; Sema3aa and Sema3ab are expressed within the somites and this restricts ISV development to the intersomitic boundaries (Childs et al., 2002; Torres-Vázquez et al., 2004). In addition, the development of the zebrafish common cardinal vein, which requires collective endothelial cell migration, is guided by repulsive cues provided by Sema3d and Plxnd1 signalling (Hamm et al., 2016). Knockdown of mouse *Plxnd1* demonstrated that it also has a role in lymphatic development. SEMA3G, which is expressed by dermal arteries, provides a repulsive cue to PLXND1-expressing LECs and knockout of either PLXND1 or SEMA3G results in the dermal lymphatics being aligned more closely with dermal blood vessels (Liu et al., 2016). PLXND1 mutants have additional lymphatic precursors in the intersomitic vessels and display extra branching in the developing cardiac lymphatics (Maruyama et al., 2021; Yang et al., 2012).

In this study, we show that loss of zebrafish Plxnd1 function results in misguided ISLVs, aberrant branching of the facial lymphatics and an increase in the number of facial LECs. Together, our data shows that Plxnd1 transduces repulsive Sema3 signals to guide lymphatic vessels and limit lymphangiogenesis, and is therefore a potential pathway that can be manipulated to control lymphatic vessel growth.

RESULTS

plxnd1 mutants have uncontrolled lymphatic vessel growth

We conducted a forward genetic screen in the lymphatic-marking *lyve1b:DsRed* transgenic zebrafish line (Okuda et al., 2012) with the aim of identifying genes that regulate lymphatic vessel development. From this screen, we identified a recessive mutant (*nz75*) that displayed non-stereotypical growth of the lymphatics in the trunk and the head (Fig. 1) – a phenotype that had not been previously described in zebrafish lymphatic mutants. Mutants were

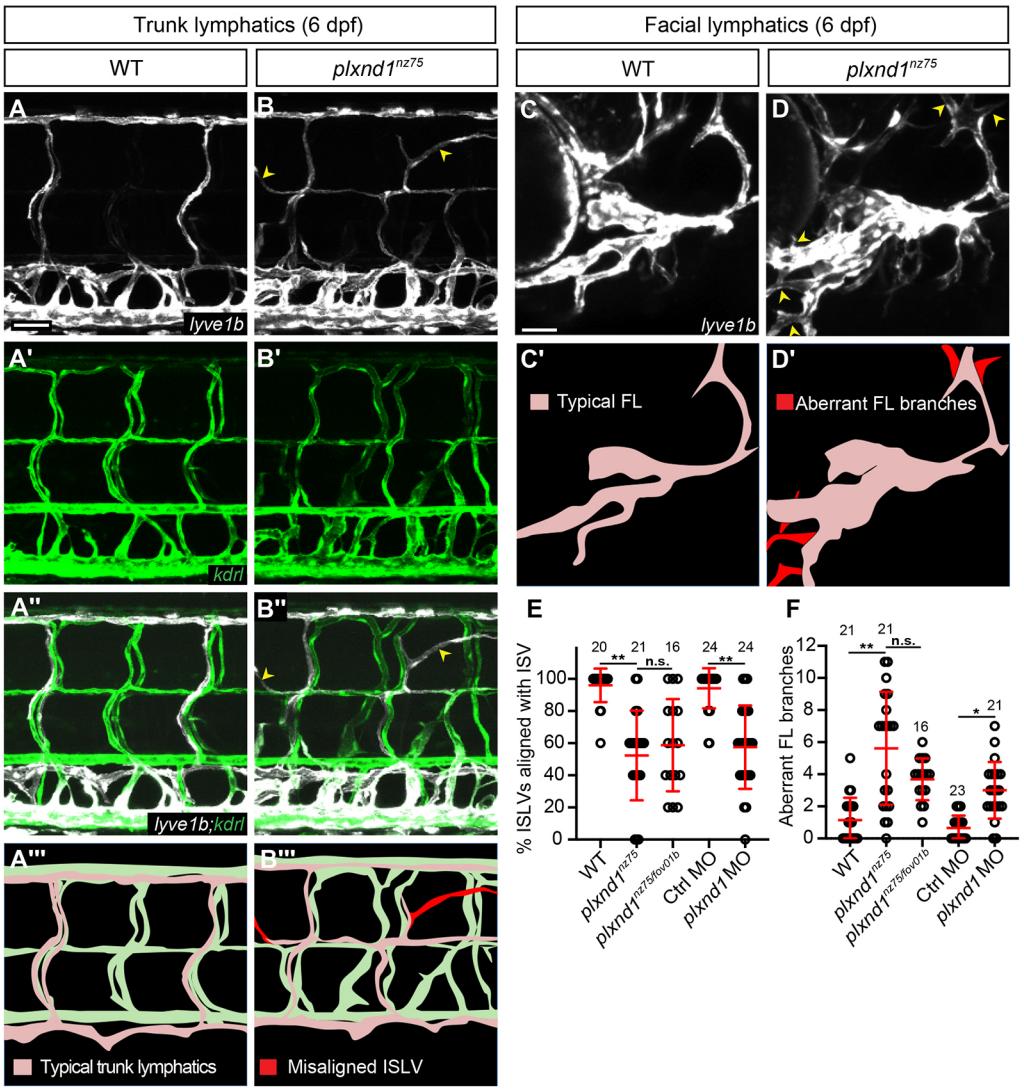

Fig. 1. *plxnd1* mutants have misaligned ISLVs and aberrant facial lymphatic branches. (A-D′) Confocal images of the trunk (A-A″,B-B″) and facial (C,D) lymphatics in *lyve1b:DsRed* (white); *kdrl:EGFP* (green) larvae at 6 dpf. Yellow arrowheads indicate ISLVs that are not aligned with an ISV (B,B″) or aberrant facial lymphatic branches (D) in *plxnd1*^{nz75} larvae. For clarity, EGFP-positive vessels in the head are not displayed. Schematics highlight the misaligned ISLVs (A‴,B‴) or aberrant facial lymphatics (C′,D′) in each corresponding confocal image. (E,F) Quantitation of the number of misaligned ISLVs (E) and aberrant facial lymphatic branches (F). P>0.05 (n.s., not significant), *P<0.05, **P<0.01 (Brown-Forsythe, and Welch ANOVA and Kruskal–Wallis test); data are mean±s.d. Scale bars: 50 µm. ISLV, intersegmental lymphatic vessel. Numbers in graphs represent numbers of larvae.

Development (2022) 149, dev200560. doi:10.1242/dev.200560

viable and fertile as adults, and displayed no gross abnormalities (Fig. S1).

Using whole-genome sequencing coupled with SNP homozygosity linkage analysis (Leshchiner et al., 2012), we mapped the causative mutation to a 600 kb region at the telomeric region of chromosome 8. Within this region was *plxnd1*, which had been previously implicated in blood vessel guidance and was therefore a clear candidate (Fig. S1). Sequencing the coding regions of *plxnd1* in the mutant revealed a single nucleotide substitution of thymine to guanine, resulting in an amino acid change from isoleucine to serine in residue 1030 within the third IPT domain of Plxnd1 (Fig. S1). This residue is highly conserved, and secondary structure prediction revealed that this mutation is likely to destabilize β-sheet formation, leading to a reduction of function (Fig. S1).

Plxnd1 has previously been shown to regulate blood vessel development, with the *out of bounds* (*plxnd1*^{fov01b}) mutant displaying aberrant intersegmental blood vessel (ISV) growth (Childs et al., 2002; Torres-Vázquez et al., 2004). Consistent with this, our *plxnd1*^{nz75} mutants displayed a phenotype of abnormally patterned intersegmental blood vessels (ISVs). In wild-type animals, the primary ISVs emerged from the DA at the intersomitic boundaries and had no additional branches emerging from the main ISV (Fig. S2). In contrast, *plxnd1*^{nz75} mutant fish displayed aberrant ISVs emerging at various locations across the DA and each ISV had sub-branches (Fig. S2). This phenotype was also observed in wild-type fish subjected to morpholino-mediated *plxnd1*-knockdown. The blood vessel phenotype was quantitated using two measures. Aberrant ISVs were defined as any ISV arising from the DA in a mid-somitic position. The second involved counting the number of branchpoints for each ISV at 36 hpf. *plxnd1*^{nz75} mutant fish both displayed a 10-fold increase in the number of aberrant ISVs and 11-fold increase in ISV branchpoints (Fig. S2). Although a similar phenotype was observed in both *plxnd1* morphants and *plxnd1*^{fov01b} mutants, the severity of the ISV branching phenotype was significantly higher in both the *plxnd1*^{fov01b} mutant and *plxnd1* morphants (18-fold increase in morphants, 16-fold in *fov01b* mutants versus 11-fold in *nz75* mutants), suggesting that the *plxnd1*^{nz75} allele is a partial loss of function (Fig. S2). Importantly, *plxnd1* mutant and morphant embryos displaying this blood vessel phenotype completely segregated with the previously observed lymphatic phenotype (Fig. 1) suggesting that *plxnd1* is responsible for both blood and lymphatic vessel patterning.

Plxnd1 regulates secondary angiogenic sprouting

We and others have demonstrated that there is an increase in primary angiogenesis (sprouting from the DA) in *plxnd1*^{nz75} mutants and morphants (Fig. S2) (Torres-Vázquez et al., 2004), but the role of Plxnd1 signalling in secondary angiogenesis (sprouting from the PCV) was unknown. In order to investigate this, we imaged *lyve1b:EGFP* larvae at 39 hpf – a timepoint when secondary sprouts are emerging from the PCV – and observed an ∼1.5-fold increase in secondary angiogenic sprouts in both *plxnd1*^{nz75} mutants and morphants (Fig. S3). Normally, half of these secondary sprouts contribute to the trunk lymphatic network by migrating to form parachordal LECs (PLs) at the horizontal myoseptum, while the other half anastomose with nearby ISVs to create veins (Geudens et al., 2019; Hogan et al., 2009b). We therefore examined both PL formation at 48 hpf as well as the number and ratio of arterial and venous ISVs in both *plxnd1*^{nz75} mutants and morphants. Surprisingly, we found no increase in PL number in either *plxnd1*^{nz75} mutants or morphants (Fig. S3). Instead, we found that there was an approximate twofold increase in the number of venous ISVs, which, because of the corresponding earlier increase in primary sprouting (Fig. S2) resulted in a twofold increase in arterial ISVs, and a 1:1 arterial:venous ratio in 72 hpf *plxnd1* animals (Fig. S3). These data indicate that the additional secondary sprouting in *plxnd1* mutants contributes towards the trunk blood vascular network.

Plxnd1 acts as a lymphatic guidance factor

We noted that there were mispatterned intersegmental lymphatic vessels (ISLVs) in *plxnd1*^{nz75} mutants and morphants at 6 dpf (Fig. 1A-F). The ISLVs are typically guided during their development by growing along arterial ISVs (aISVs) and therefore the pattern of ISLV growth is normally congruent with the underlying pattern of aISVs (Bussmann et al., 2010). There are two explanations for the mispatterned ISLVs we observed in *plxnd1*^{nz75} animals. The first is that the ISLVs are mispatterned indirectly, owing to the ISV defect induced by loss of *plxnd1* (Fig. S2), in which case the lymphatics will still align with the ISVs. The second is that *plxnd1* is directly required for ISLV guidance, in which case the lymphatics will develop independently of the ISVs. To distinguish between these two possibilities, we quantitated the percentage of ISLVs that did not align with an ISV in double transgenic *lyve1b:DsRed; kdrl:EGFP* larvae. Whereas wild-type and control morpholino-treated larvae almost never displayed ISLVs that were misaligned with ISVs (96% and 94% ISLV-ISV alignment, respectively), ISLVs were frequently observed in both *plxnd1*^{nz75} mutants and in morphants developing separate from the ISVs (52% and 58% ISLV-ISV alignment, respectively), suggesting that *plxnd1* is directly required for correct ISLV patterning (Fig. 1E). *plxnd1*$^{nz75/fov01b}$ trans-heterozygotes also displayed an increase in misaligned ISLVs (59% ISLV-ISV alignment) (Fig. 1E), confirming that the ISLV misguidance phenotype was caused by loss of *plxnd1*.

We further examined the facial lymphatic phenotype at 6 dpf in *plxnd1*^{nz75} mutants and in *plxnd1* morphants. Any facial lymphatic branches that are not usually observed in wild-type animals were considered aberrant. We noted that *plxnd1* animals frequently displayed aberrant branches from vessels within the facial lymphatic network (Fig. 1C,D). Quantitation revealed that *plxnd1*^{nz75} mutants had a fivefold increase in the number of aberrant facial lymphatic branches (Fig. 1F) suggesting that *plxnd1* normally prevents excessive facial lymphatic growth. *plxnd1*$^{nz75/fov01b}$ trans-heterozygotes also displayed a threefold increase in aberrant facial lymphatic branches (Fig. 1F), confirming that this phenotype was caused by the loss of *plxnd1*.

To further confirm the ISLV misguidance phenotype, we examined ISLV patterning in *soluble flt1* (*sflt1*) morphants. sFlt1 normally inhibits blood vessel growth by binding and sequestering Vegfa ligands; therefore, knockdown of this gene is known to cause aberrant growth of ISVs, but sFlt1 is not able to bind either Vegfd or Vegfc, and is not predicted to directly influence ISLV growth (Krueger et al., 2011; Vogrin et al., 2019). A previously validated *sflt1* splice-blocking morpholino (Krueger et al., 2011; Wild et al., 2017) was injected into *lyve1b:DsRed; kdrl:EGFP* fish and the blood and lymphatic vessels in the trunks of these larvae were imaged at 6 dpf. Despite the expected 11-fold increase in ISV branching, there was no accompanying increase in misaligned ISLVs in *sflt1* morphants (Fig. S4). This demonstrates that ectopic ISV growth is not sufficient to uncouple ISLV guidance from the ISVs, and provides further evidence for the direct guidance of ISLV growth by Plxnd1.

Development (2022) 149, dev200560. doi:10.1242/dev.200560

We examined the ISLV misguidance phenotype in detail by performing time-lapse imaging of both wild-type (Movie 1) and *plxnd1*^{nz75} (Movie 2) animals from 60 to 70 hpf – when the parachordal LECs normally migrate from the horizontal myoseptum (HM) to form ISLVs alongside adjacent aISVs (Bussmann et al., 2010). In wild-type larvae, the developing ISLVs began migrating from the HM at the junction with each aISV but in *plxnd1*^{nz75} larvae, the developing ISLVs would frequently migrate out of the HM at other locations (Fig. 2A-J). Furthermore, whereas wild-type ISLVs spent almost 100% of their migration path aligned with aISVs, in *plxnd1*^{nz75} larvae they spent only 60% of their time in contact with an artery (Fig. 2K). Consequently, the developing ISLVs in *plxnd1*^{nz75} larvae often deviate from the ventral-to-dorsal growth trajectory characteristic of wild types, instead growing in an anterior or posterior direction, as shown by the traces displaying the ISLV growth paths (Fig. 2I,J). Finally, whereas in wild-type larvae the developing ISLV generally had a single growing tip and therefore one direction of migration, in *plxnd1*^{nz75} larvae the developing ISLVs were frequently observed to have multiple tips, with a fourfold increase in branching events per hour (Fig. 2L). The vessel tips would also frequently regress and change direction, taking a tortuous path to reach their final position, as seen by the 1.8-fold increase in ISLV meandering behaviour in *plxnd1*^{nz75} larvae (Fig. 2M). Taken together, these data show that Plxnd1 normally functions to restrict lymphatic vessel migration to ensure the stereotypical pattern of the trunk and head lymphatic networks.

Plxnd1 acts cell autonomously to regulate lymphatic vessel guidance

Our data indicate that Plxnd1 signalling regulates lymphatic vessel guidance. To test whether Plxnd1 performs this role in a cell-autonomous fashion, we first confirmed that *plxnd1* is expressed in developing zebrafish lymphatic vessels by performing whole-mount *in situ* hybridisation. We observed *plxnd1* expression in the trunk blood vasculature at 36 hpf, as shown previously (Fig. S5) (Torres-Vázquez et al., 2004). In *lyve1b:EGFP* embryos at 48 hpf – a timepoint when the developing facial and trunk lymphatics can be visualised using an anti-*EGFP* probe (Okuda et al., 2012), we observed *plxnd1* expression in both the facial lymphatic sprout in the head and in the parachordal LECs in the trunk, confirming that *plxnd1* is expressed in zebrafish LECs during lymphatic vessel development (Fig. 3A,B, Movies 3 and 4).

Next we investigated whether Plxnd1 acts cell autonomously within LECs. In order to test this hypothesis, transplantations were performed between *plxnd1*^{nz75} donors and wild-type hosts at the blastula stage. If *plxnd1* acts cell autonomously to guide lymphatic growth, then *plxnd1*^{nz75} donor LECs would be expected to grow ectopically in wild-type hosts. To visualise the origin and fate of donor-derived endothelium, cells were transplanted from *lyve1b:*

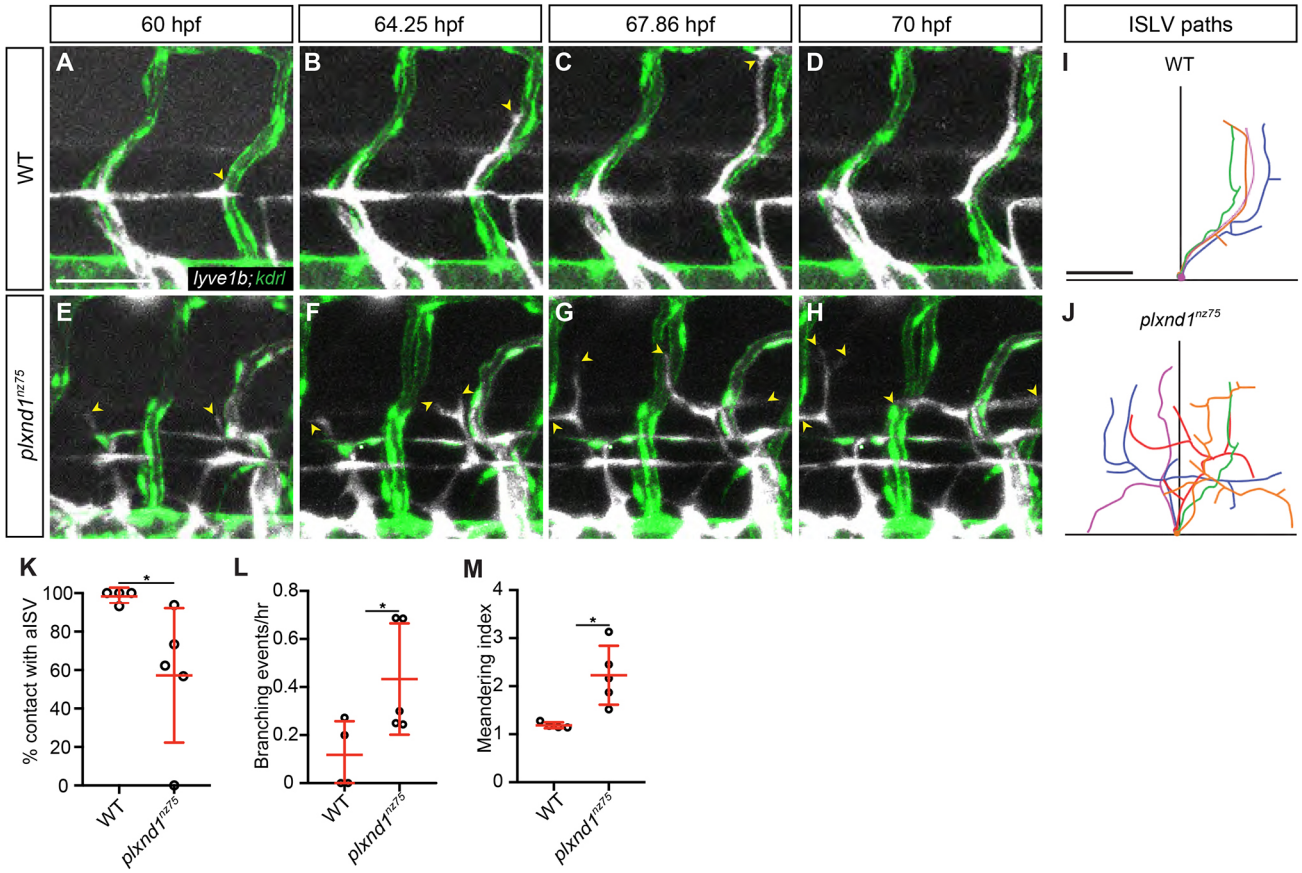

Fig. 2. *plxnd1* is required for the alignment of developing ISLVs to blood vessels. (A-H) Still images from time-lapse movies of ISLV growth between 60 and 70 hpf in *lyve1b:DsRed; kdrl:EGFP* wild type (A-D) and *plxnd1*^{nz75} (E-H) larvae showing blood vessels (green) *lyve1b*-expressing vessels (white) from Movies 1 and 2, respectively. Yellow arrowheads indicate the distal tip of each ISLV. (I,J) Traces of ISLV growth paths for wild type (I) and *plxnd1* (J) (n=4). ISLVs were traced dorsally from when they left the horizontal myoseptum. (K) Quantitation of the percentage of time the ISLVs are aligned with a blood vessel (n=4). (L) Quantitation of the number of ISLV branching events (n=4). (M) Quantitation of the ISLV meandering index (n=4). *P<0.05 (Mann–Whitney test); data are mean±s.d. Scale bar: 50 µm. ISLV, intersegmental lymphatic vessel.

Development (2022) 149, dev200560. doi:10.1242/dev.200560

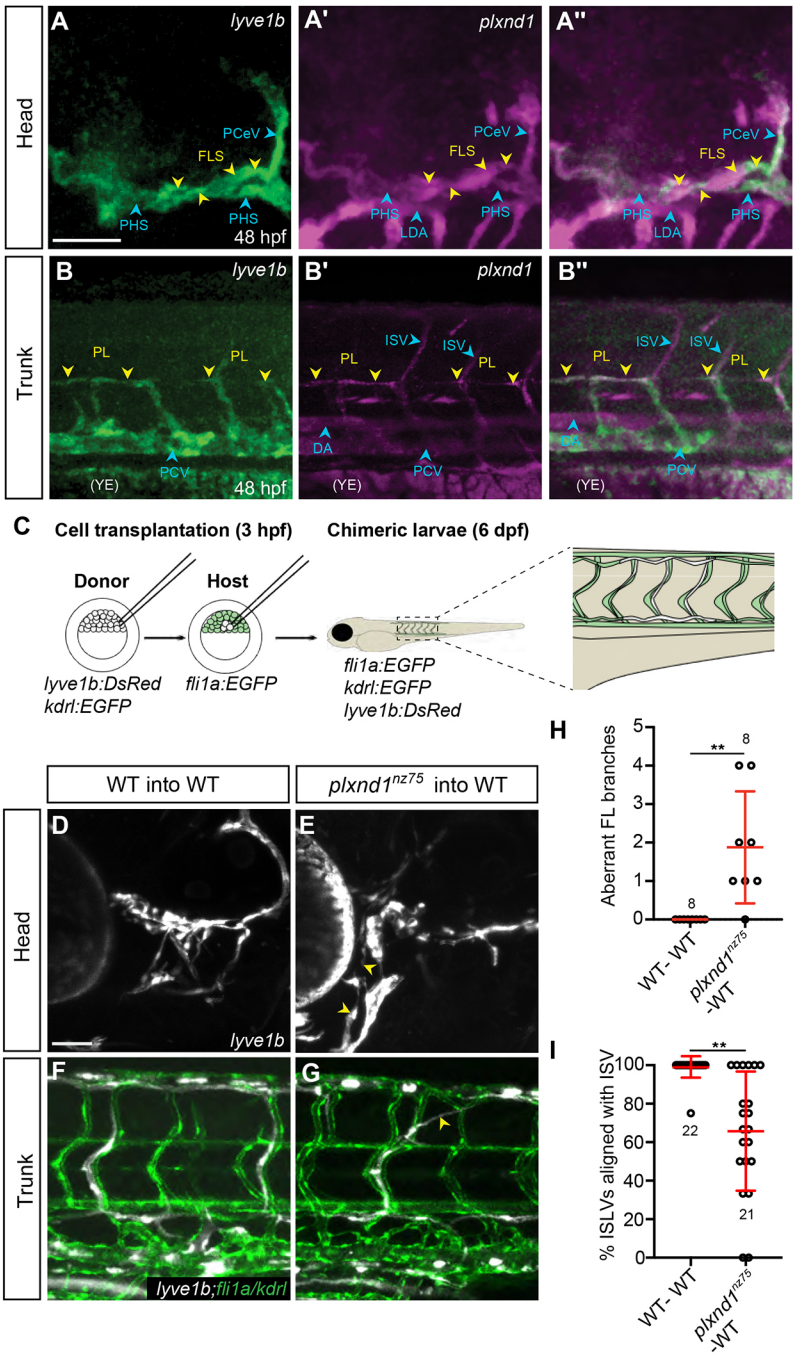

Fig. 3. *plxnd1* acts cell-autonomously to guide lymphatic vessel growth. (A-B″) Confocal images of the *lyve1b:EGFP* expression (anti-EGFP, green) (A,B), *plxnd1* expression (anti-*plxnd1*, magenta) (A′,B′) or both (A″,B″) in the head (A,A″) or trunk (B,B″) of 48 hpf *lyve1b:EGFP* larvae. Yellow arrowheads indicate either the facial lymphatic sprout (A) or the parachordal LECs (B). Blue arrowheads indicate blood vessels. There is non-specific staining in the yolk extension (YE). (C) Schematic of the transplantation protocol. Cells were transplanted from 3 hpf *lyve1b:DsRed; kdrl:EGFP* donor embryos to 3 hpf *fli1a:EGFP* host embryos, resulting in chimeric larva with host-derived blood and lymphatic vessels indicated in light green and donor-derived lymphatic vessels indicated in white. (D,E) Confocal images of the facial vasculature in chimeric animals at 6 dpf showing donor-derived LECs (white) from either wild-type (D) or *plxnd1*^{nz75} (E) donors. For clarity, EGFP-positive vessels are not displayed. Aberrant *plxnd1*^{nz75} facial lymphatic vessels are highlighted by yellow arrowheads in E. (F,G) Confocal images of the trunk vasculature in chimeric animals at 6 dpf showing donor-derived LECs (white) from either wild-type (F) or *plxnd1*^{nz75} (G) donors. Note the misaligned *plxnd1*^{nz75} vessel highlighted by the yellow arrowhead in G. (H,I) Quantitation of aberrant facial lymphatics (H) or the number of misaligned ISLVs (I) at 6 dpf. ***P*<0.01 (Mann–Whitney test); data are mean±s.d. Scale bars: 50 µm. DA, dorsal aorta; FLS, facial lymphatic sprout; ISV, intersegmental vessel; ISLV, intersegmental lymphatic vessel; LDA, lateral dorsal aorta; PCV, posterior cardinal vein; PCeV, posterior cerebral vein; PL, parachordal LEC; PHS, primary head sinus; YE, yolk extension. Numbers in graphs represent numbers of larvae.

DsRed; kdrl:EGFP donor embryos into *fli1a:EGFP* host embryos (Fig. 3C). The expression of DsRed in the host embryos allowed the visualisation of donor-derived LECs at 6 dpf, while EGFP expression allowed visualisation of both host (*fli1a:EGFP*) and donor-derived (*kdrl:EGFP*) blood ECs at 6 dpf. In this way, it could be determined whether donor LECs are being guided normally by growing along blood vessels or whether they are misaligned with either host- or donor-derived blood ECs. The transplants were conducted using donor and host blastula embryos at 3 hpf. Chimeric embryos were raised and the facial and trunk vasculature imaged at 6 dpf.

As expected, wild-type LECs in wild-type hosts did not form aberrant branches in the facial lymphatics and did not result in misaligned ISLVs (Fig. 3D,F,H,I). In contrast, *plxnd1*^{nz75} LECs in wild-type hosts displayed an 1.8-fold increase in the number of aberrant branches from *plxnd1*^{nz75} (*lyve1b:DsRed*-expressing) facial vessels. In the trunk, only 66% of *plxnd1*^{nz75} (*lyve1b:DsRed*-expressing) ISLVs were correctly aligned with aISVs, compared with 99% of wild-type (*fli1a:EGFP*-expressing) host ISLVs (Fig. 3E,G,H,I). Finally, there was a ninefold increase in aberrant ISV growth in the *plxnd1*^{nz75} mosaic animals, which was consistent with the role of *plxnd1* in regulating ISV migration (Childs et al., 2002; Torres-Vázquez et al., 2004) (Fig. S5). Overall, our results indicate that *plxnd1* is acting cell-autonomously within LECs to guide lymphatic vessel growth.

Plxnd1 antagonises Vegfr signalling to regulate facial lymphatic growth

We also noted an additional phenotype in the facial lymphatics of our *plxnd1*^{nz75} mutant and morphants. At 6 dpf, the facial lymphatics appeared thickened, with enlarged LFLs, MFLs

Development (2022) 149, dev200560. doi:10.1242/dev.200560

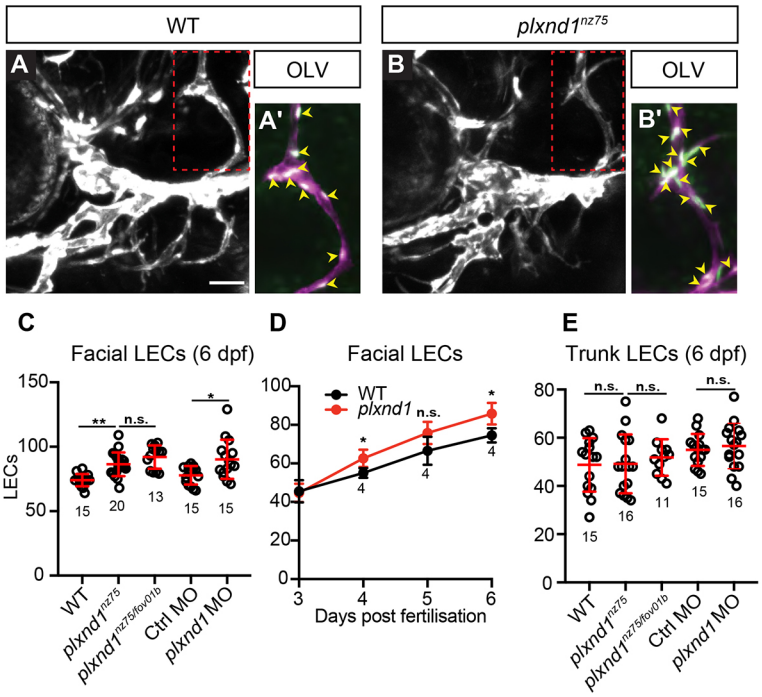

Fig. 4. *plxnd1* mutants display facial lymphatic hyperplasia. (A,B) Confocal images of the facial vasculature showing the *lyve1b*-expressing vessels (white) in 6 dpf *lyve1b:DsRed; fli1a:nlsEGFP* wild-type (A) or *plxnd1*^{nz75} (B) larvae. (A′,B′) Areas outlined in A,B showing LECs within the OLV (*lyve1b*, magenta; *fli1a:nlsEGFP*, green). Yellow arrowheads indicate OLV nuclei. (C) Quantitation of facial LEC number at 6 dpf. (D) Quantitation facial LEC number from 3 to 6 dpf. (E) Quantitation of trunk LEC number at 6 dpf. P>0.05 (not significant), *P<0.05, **P<0.01 (one-way ANOVA); data are mean±s.d. Scale bar: 50 µm. LEC, lymphatic endothelial cell; OLV, otolithic lymphatic vessel. Numbers in graphs represent numbers of larvae.

and OLVs when compared with controls – suggesting an increase in the number of facial LECs. To test this, we generated double transgenic *lyve1b:DsRed; fli1a:nlsEGFP* fish and counted the number of facial LECs (fLECS) present at 6 dpf. This revealed that the *plxnd1*^{nz75} mutants and morphants had ∼16% more fLECs than controls (Fig. 4A-C). This phenotype was also observed in *plxnd1*$^{nz75/fov01b}$ trans-heterozygotes (24% increase in fLECs over wild type), confirming that the loss of PLXND1 signalling results in facial lymphatic hyperplasia. To define when facial lymphatic hyperplasia occurs in the mutants, wild type and *plxnd1*^{nz75} larvae were imaged at 3, 4, 5 and 6 dpf, with the *plxnd1*^{nz75} larvae displaying significantly more facial LECs at 4 and 6 dpf (Fig. 4D). Next, we examined the numbers of *prox1a*-expressing lymphatic progenitors in the head and observed no difference between *plxnd1*^{nz75} mutants and wild type (Fig. S6). Taken together, these data show that the facial lymphatic hyperplasia in *plxnd1*^{nz75} animals occurs after lymphatic specification and sprouting. We also quantitated trunk LECs at 6 dpf, as well as *prox1a*-expressing lymphatic progenitor formation in the PCV at 36 hpf, and found no evidence of either trunk lymphatic hyperplasia or an increase in lymphatic progenitors (Fig. 4E, Fig. S6) – a result consistent with our earlier analysis showing normal numbers of parachordal LECs in *plxnd1*^{nz75} animals (Fig. S3).

We next determined whether the facial lymphatic hyperplasia phenotype depends on Vegfr signalling. To test this, we used two small molecule inhibitors – sunitinib (a tyrosine kinase inhibitor) and tivozanib (a specific VEGFR inhibitor) – that block lymphatic vessel growth in zebrafish (Okuda et al., 2015). *lyve1b:DsRed; fli1a:nlsEGFP* larvae were placed into a solution of DMSO, 1 µM sunitinib or 2 nM tivozanib at 3 dpf – a timepoint before the onset of the hyperplasia phenotype and maintained in these compounds until 6 dpf when they were analysed. These inhibitor concentrations were chosen as they are the highest doses that still allow the complete development of both the facial and trunk lymphatic networks. Drug-treated wild-type larvae displayed a modest reduction in the average number of fLECs (DMSO=78, sunitinib 60, tivozanib=64) – a result consistent with inhibition of Vegfr signalling, whereas inhibitor treatment of *plxnd1*^{nz75} larvae was able to rescue the facial lymphatic hyperplasia by normalising facial LEC numbers (*plxnd1*+DMSO=88, *plxnd1*+sunitinib=63, *plxnd1*+tivozanib=70). This rescue suggests that elevated Vegfr signalling drives the facial lymphatic hyperplasia phenotype seen in *plxnd1*^{nz75} larvae (Fig. 5A). Of note, when the same level of Vegfr inhibition was applied from 2 to 6 dpf it had no significant effect on either the number of aberrant facial lymphatic branches or in the degree of misalignment of the ISLVs at 6 dpf, suggesting that dysregulated Vegfr signalling is not responsible for the misguidance of lymphatics in *plxnd1*^{nz75} mutants (Fig. S7).

In order to investigate which signalling pathway downstream of Vegfr is overactivated in *plxnd1* larvae, we examined the activity of the MEK/ERK pathway, as it is known to be inhibited by SEMA3/PLXND1, is downstream of VEGFR function and is also known to promote cell proliferation and survival in LECs (Baek et al., 2019; Carretero-Ortega et al., 2019; Grimm et al., 2019; Shin et al., 2016; Wortzel and Seger, 2011). Erk activity was measured by immunostaining against phospho-Erk (pErk) and anti-EGFP in 36 hpf *lyve1b:EGFP* larvae. The percentage of pErk-positive cells in the PCV of *plxnd1* morphants was increased to 61% compared with only 39% in control morphants, indicating that the higher levels of secondary sprouting seen upon the loss of Plxnd1 may be a result of increased Erk signalling within the PCV (Fig. 5B). We then investigated Erk activity in the facial lymphatics at 3 dpf (Fig. 5C-E) and observed a significant increase in the proportion of pErk-positive fLECs in *plxnd1* morphants (36% of fLECs were pErk-positive) over control morphants (20% of fLECs were pERK-positive) (Fig. 5C-E). To test the role of the Mek/Erk pathway in facial lymphatic hyperplasia phenotype, wild-type and *plxnd1*^{nz75} larvae were treated with 5 µM of the MEK inhibitor SL327 from 3 to 6 dpf. This dose was chosen as it is the highest possible dose that still allows the complete development of the facial lymphatic network. Inhibition of Mek signalling was able to rescue the facial lymphatic hyperplasia phenotype in *plxnd1*^{nz75} larvae,

Development (2022) 149, dev200560. doi:10.1242/dev.200560

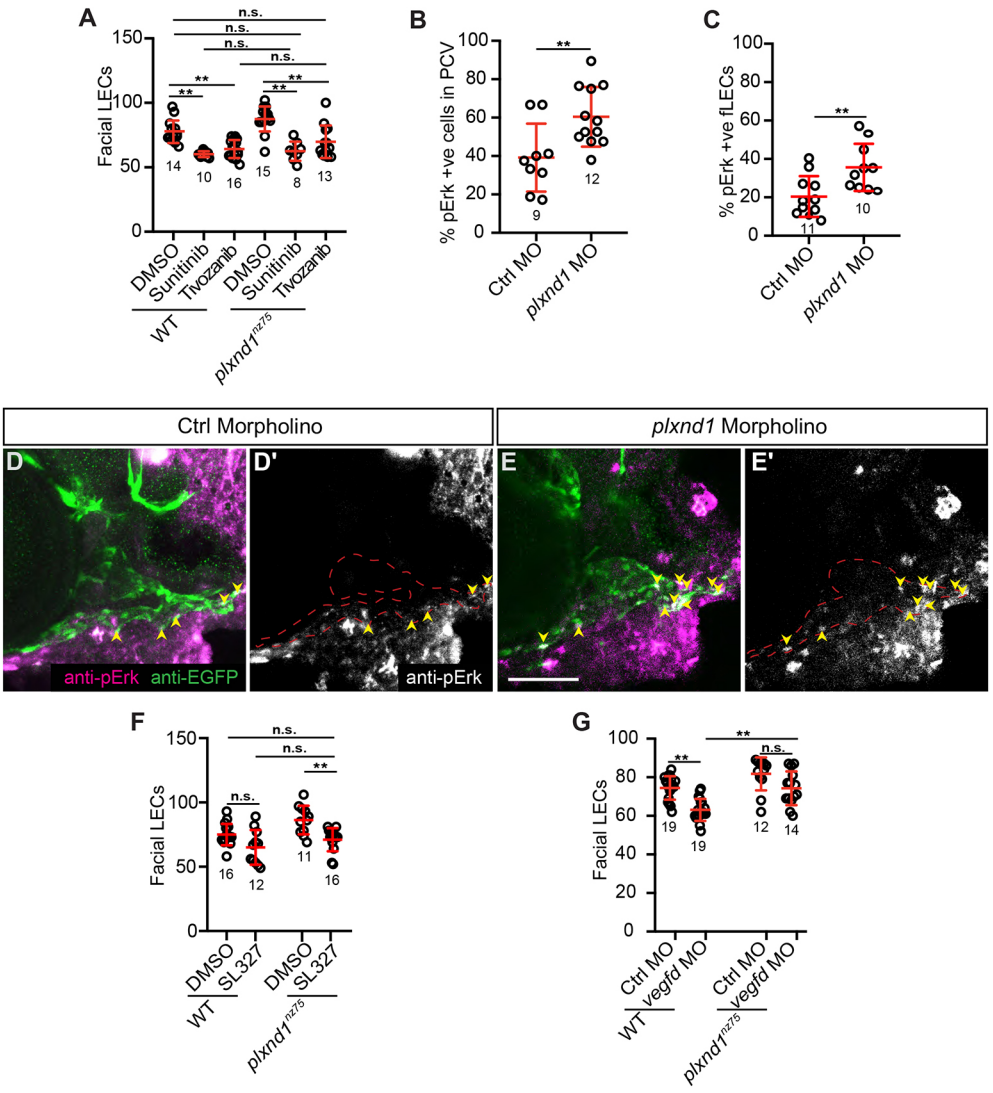

Fig. 5. *plxnd1* mutants have elevated Vegfr/Erk signalling in the facial lymphatics. (A) Quantitation of facial LEC number in 6 dpf larvae treated from 3 to 6 dpf with either DMSO, 1 µM sunitinib or 2 nM tivozanib. (B,C) Quantitation of the proportion of pErk-positive cells within the PCV at 36 hpf (B) or the facial LECs at 3 dpf (C). (D-E′) Confocal images of anti-pErk (magenta) and anti-EGFP (green) staining in the head at 3 dpf of either control (D,D′) or *plxnd1* (E,E′) *lyve1b:EGFP* morphant larvae. (D′,E′) Anti-pErk staining only. Yellow arrowheads indicate the pErk cells within the facial lymphatics. (F) Quantitation of facial LEC number in 6 dpf larvae treated from 3 to 6 dpf with either DMSO or 5 µM SL327. (G) Quantitation of facial LEC number in *lyve1b:DsRed; fli1a:nlsEGFP* larvae injected with either control or *vegfd* morpholinos. $P>0.05$ (not significant), $^{*}P<0.05$, $^{**}P<0.01$ (unpaired *t*-tests, Kruskal–Wallis and ANOVA); data are mean±s.d. Scale bar: 50 µm. LEC, lymphatic endothelial cell. Numbers in graphs represent numbers of larvae.

with fLEC number reduced to wild-type levels (WT+DMSO=75, *plxnd1*^{nz75}=86, *plxnd1*^{nz75}+SL327=71) (Fig. 5F), indicating that Plxnd1 signalling normally antagonises Vegfr signalling through the Mek/Erk pathway in order to limit fLEC numbers.

It was intriguing that lymphatic hyperplasia was observed only in the facial lymphatic network. One of the key differences between facial and trunk lymphatic development is that the facial lymphatics require Vegfd-induced Kdr signalling (Astin et al., 2014a; Bower et al., 2017; Vogrin et al., 2019). We hypothesised that Plxnd1 might normally antagonise Kdr-driven Erk signalling, which results in a specific facial lymphatic hyperplasia phenotype when *plxnd1* is lost. As Vegfd can only bind to Kdr (Vogrin et al., 2019), we predicted that *plxnd1* mutants should be resistant to *vegfd* knockdown. To test this, *lyve1b:DsRed; fli1a:nlsEGFP* wild-type or *plxnd1*^{nz75} embryos were injected with either control morpholino or a previously validated *vegfd* morpholino (Astin et al., 2014a; Bower et al., 2017) and the fLECs were quantified. We found that, as expected, *vegfd* knockdown resulted in a 15% reduction in fLECs in wild-type larvae but, by contrast, there was no significant reduction in fLEC numbers in *plxnd1*^{nz75} mutants (Fig. 5G). Taken together, these data suggest that Plxnd1 signalling normally antagonises Kdr-driven Mek/Erk signalling to limit fLEC numbers.

Sema3 ligands regulate trunk lymphatic development

Plxnd1 is thought to negatively regulate ISV growth through the ligands Sema3aa and Sema3ab (Torres-Vázquez et al., 2004). These secreted Sema ligands are expressed from the somites where they could bind to and activate Plxnd1 signalling in the blood endothelial cells to prevent aberrant growth of the ISVs into the adjacent somites (Torres-Vázquez et al., 2004). Given the similarity in phenotype between the blood and lymphatic misguidance phenotypes in the trunk, we wondered whether these ligands may also be required for ISLV guidance. We first confirmed that both *sema3aa* and *sema3ab* are expressed in the somites by whole-mount *in situ* hybridisation at 24 hpf. Although we were unable to observe a reliable *in situ* signal for either gene at 30 or 48 hpf, RT-PCR confirmed that both of these genes are expressed in both the head and trunk at 48 hpf during lymphatic development (Fig. S8).

We analysed a *sema3aa*^{sa10241} mutant generated by The Zebrafish Mutation Project (Kettleborough et al., 2013). This mutant contains a C-to-T substitution that converts Gln501 into a premature stop codon, truncating the protein by 359 amino acids within the semaphorin domain. We observed a significant increase in the frequency of misaligned ISLVs in *sema3aa*^{sa10241} mutant embryos when compared with wild type (wild type=95% ISLV-ISV alignment, *sema3aa*=78% ISLV-ISV alignment) (Fig. 6A-G),

Development (2022) 149, dev200560. doi:10.1242/dev.200560

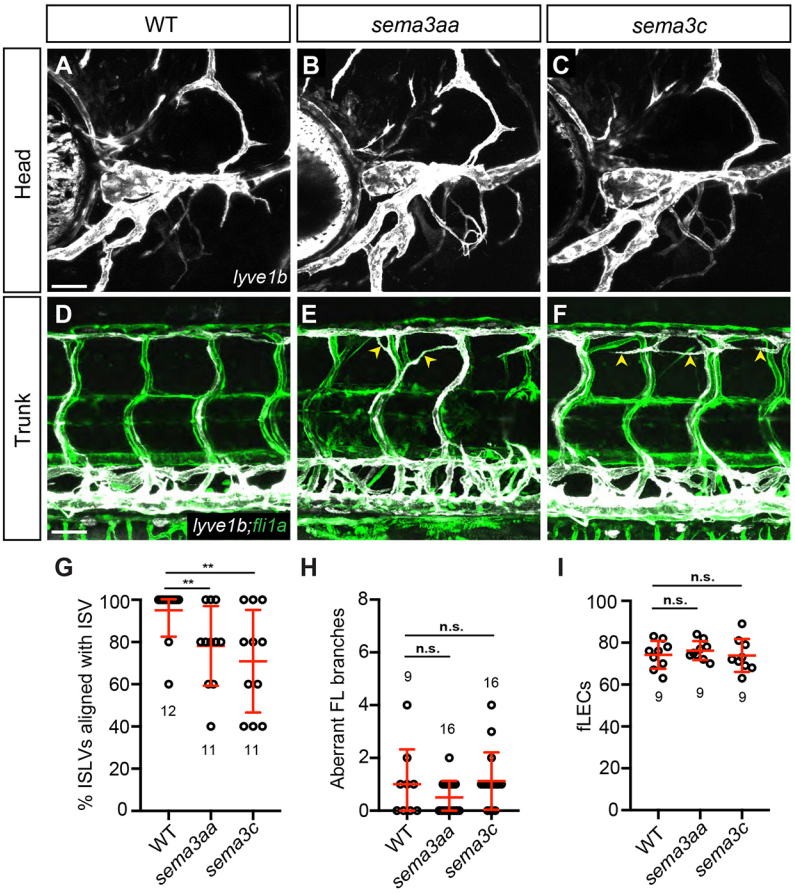

Fig. 6. Semaphorin 3 ligands regulate trunk lymphatic guidance. (A-F) Confocal images of the head (A-C) or trunk (D-F) vasculature showing the blood (green) and *lyve1b*-expressing vessels (white) in 6 dpf *lyve1b:DsRed; fli1a:EGFP* wild type (A,D) and *sema3aa*^{sa10241} (B,E) or *sema3c*^{sa15161} (C,F) mutants. Yellow arrowheads indicate misaligned ISLVs. (G) Quantitation of misaligned ISLVs at 6 dpf. (H) Quantitation of aberrant facial lymphatics at 6 dpf. (I) Quantitation of facial LEC number at 6 dpf. $P>0.05$ (not significant), $^{**}P<0.01$ (by Mann–Whitney test); data are mean±s.d. Scale bar: 50 µm. ISLV, intersegmental lymphatic vessel. Numbers in graphs represent numbers of larvae.

demonstrating that Sema3aa ligands are involved in the Plxnd1-mediated guidance of ISLV growth. However, *sema3aa*^{sa10241} mutants had no increase in aberrant facial lymphatic branches or in the number of fLECs (Fig. 6B,H,I), suggesting that the role of this ligand is restricted to the trunk lymphatic development.

Sema3c has been previously shown to be expressed in the head during facial lymphatic development (Callander et al., 2007; Yu and Moens, 2005) and was therefore a candidate Plxnd1 ligand to be involved in facial lymphatic growth and guidance. Whole-mount *in situ* hybridisation at 24 and 30 hpf showed that *sema3c* was also expressed in neuronal cells in the trunk and RT-PCR from both head and trunk RNA confirmed that expression was maintained in both the head and trunk at 48 hpf during lymphatic vessel development (Fig. S8). A *sema3c*^{sa15161} mutant generated by The Zebrafish Mutation Project (Kettleborough et al., 2013) was obtained. This mutant contains a C-to-A substitution that converts Ser142 and Ser186 in the 713 and 757 amino acid Sema3c isoforms into a premature stop codon, thus truncating these proteins within the semaphorin domain. We observed a significant increase in misaligned ISLVs in the trunk of *sema3c*^{sa15161} mutants (wild type=95% ISLV-ISV alignment, *sema3c*=70% ISLV-ISV alignment) (Fig. 6D-G), demonstrating that multiple Sema3 ligands are involved in the guidance of ISLV growth. However, *sema3c* mutants had no facial lymphatic defects (Fig. 6C,H,I), suggesting that *sema3c* is not required for facial lymphatic development.

DISCUSSION

We have shown that Plxnd1 acts cell autonomously in LECs to guide the pathfinding of the facial and trunk lymphatic networks (Fig. 7). In addition, we uncovered a role for *plxnd1* as a negative regulator of facial lymphangiogenesis. We show that loss of *plxnd1* results in facial lymphatic hyperplasia and that Plxnd1 normally antagonises Vegfr/Erk signalling to ensure the correct number of facial LECs (Fig. 7).

In the zebrafish trunk, the ISLVs are normally aligned with the aISVs (Bussmann et al., 2010). This interaction is, in part, mediated by chemokine signalling; Cxcl12b ligands, which are secreted from aISVs and associated mural cells, activate signalling in the Cxcr4a/b-expressing LECs that helps to anchor their migration along the aISV (Cha et al., 2012; Peng et al., 2022). We show that the loss of Plxnd1 function results in growth of ISLVs away from the blood vessels and across the somites. Live imaging revealed that growing ISLVs in *plxnd1* larvae were more dynamic, spent significantly less time aligned with aISVs and, in some instances, even migrated directly across them. This suggests that the negative guidance provided by Plxnd1 signalling is the dominant guidance cue for the correct patterning of ISLVs.

We have also identified two Sema ligands involved in ISLV guidance; *sema3aa* mutants and *sema3c* mutants both displayed misguided ISLVs similar to those observed in *plxnd1* mutants. We have confirmed that *sema3aa* is expressed in somites before lymphatic development (Torres-Vázquez et al., 2004) and that its expression is maintained in the trunk from 22 to 48 hpf. We have also shown that *sema3c* is expressed within the trunk at 48 hpf and observed expression in trunk neuronal structures by *in situ* hybridisation at 24-30 hpf. It is therefore likely that the expression of Sema ligands within the somitic region activates repulsive Plxnd1 signalling in LECs that grow towards the somite, restricting their growth to align with the aISVs within the intersomitic space (Fig. 7). The ISLV misguidance phenotype was less severe in both *sema3*

Development (2022) 149, dev200560. doi:10.1242/dev.200560

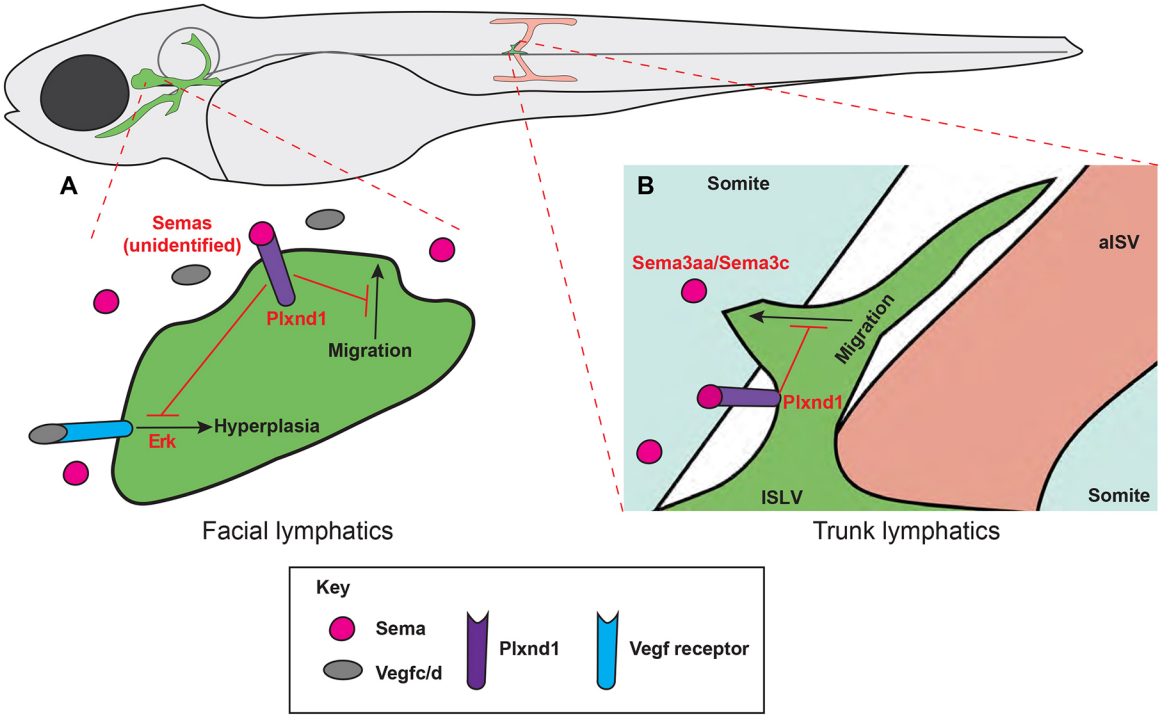

Fig. 7. Plxnd1 signalling regulates lymphatic vessel guidance and growth. Model of Plxnd1-mediatated regulation of lymphatic development. (A) In the head, Plxnd1 signalling antagonises Vegfr/Erk signalling to prevent facial lymphatic hyperplasia. It also prevents aberrant cell migration. The role and identity of semaphorin ligands in facial lymphatic development are yet to be determined. (B) In the trunk, Plxnd1 signalling within developing ISLVs, likely triggered by Sema3aa/Sema3c ligands, prevents migration into the somites.

mutants than in *plxnd1*-deficient larvae, suggesting that they act redundantly, likely with other Sema ligands (such as Sema3ab), to regulate ISLV guidance. The role of Sema3/Plxnd1 signalling in the zebrafish trunk lymphatics is similar to its role in patterning the murine lymphatics. SEMA3G ligands released by arteries have been shown to repel PLXND1-expressing dermal lymphatics (Liu et al., 2016). In addition, loss of PLXND1 causes an increase in the branching of the cardiac lymphatic plexus around the truncus arteriosus (Maruyama et al., 2021). Taken together with our data, this demonstrates that PLXND1/SEMA signalling has a conserved role in lymphatic guidance.

The facial lymphatics, which are not guided by blood vessels, were also mispatterned in *plxnd1* larvae, with an increase in aberrant branches that was similar to the phenotype observed in the trunk. Neither *sema3aa* or *sema3c* appear to be involved in facial lymphatic guidance despite both of these ligands being expressed in the head (Fig. S8) (Callander et al., 2007; Tanaka et al., 2007). The role and identity of Sema ligands involved in facial lymphatic guidance remains to be determined.

PLXND1 has a conserved role as a negative regulator of angiogenesis. It regulates blood vessel growth by antagonising VEGFR signalling and also by directly regulating cell migration through destabilising actin polymerisation and integrin-mediated cell adhesion in endothelial cells (Childs et al., 2002; Fukushima et al., 2011; Gitler et al., 2004; Gu et al., 2005; Kim et al., 2011; Maruyama et al., 2021; Moriya et al., 2010; Tata et al., 2014; Torres-Vázquez et al., 2004; Zhang et al., 2009; Zygmunt et al., 2011). We show that suppression of Vegfr signalling did not normalise the lymphatic misguidance phenotype in the trunk or the head. These data suggest that Plxnd1 inhibits pro-migration pathways that are somewhat independent of Vegfr signalling, such as actin assembly and the formation of integrin-mediated adhesions (Driessens et al., 2001; Tata et al., 2014). There are a number of intracellular modulators associated with PLXND1 signalling, such as Rho-GTPases, endocytic adaptors of the GIPC family, cytoskeletal proteins, integrins and kinases, that have been associated with PLXND1 regulation of cell growth that could be involved in lymphatic guidance (Burk et al., 2017; Carretero-Ortega et al., 2019; Choi et al., 2014; Sakurai et al., 2010, 2011; Tata et al., 2014; Uesugi et al., 2009; Wang et al., 2012). *In vitro* studies have shown that SEMA3E-PLXND1 signalling inhibits the formation of actin stress fibres and focal adhesions, which results in reduced motility and retraction of LECs (Liu et al., 2016; Maruyama et al., 2021). It is therefore possible that activation of Plxnd1 signalling causes localised disruption of the cell migration machinery, leading to withdrawal of cell protrusions and directed growth of the developing lymphatic vessel away from areas containing Sema3 ligands. Future experiments will focus on uncovering the downstream lymphatic migration pathways regulated by Plxnd1.

Plxnd1 signalling can also act as a negative regulator of lymphangiogenesis, which, unlike its guidance role, is context specific; loss of *plxnd1* caused an increase in the number of facial LECs but had no effect on trunk LECs. Unlike the misguidance phenotype, the facial lymphatic hyperplasia was normalised by suppression of either Vegfr or Mapk/Erk signalling, indicating that Plxnd1 signalling normally antagonises this pathway. In support of this, we observed an increase in Erk signalling within the fLECs of *plxnd1* morphant larvae. Plexins regulate MAP/ERK signalling in various contexts (Aurandt et al., 2006; Basile et al., 2007; Bribián et al., 2014; Ito et al., 2014). In addition, SEMA3E/PLXND1 signalling is known to inhibit VEGFR-mediated and VEGFR-independent ERK signalling in blood endothelial cells (Carretero-Ortega et al., 2019; Moriya et al., 2010) and has been shown to inhibit LEC cell proliferation (Maruyama et al., 2021; Yang et al.,

Development (2022) 149, dev200560. doi:10.1242/dev.200560

2012). However the exact molecular mechanism by which PLXND1 antagonises VEGFR signalling has not yet been established.

One of the key differences between trunk and facial lymphatic development is the specific requirement for Vegfd/Kdr signalling in the development of the facial lymphatics (Astin et al., 2014a; Bower et al., 2017; Vogrin et al., 2019). We therefore hypothesised that Plxnd1 limits Kdr signalling, and thus inactivation of *plxnd1* leads to facial lymphatic hyperplasia. In support of this, *plxnd1*^{nz75} animals were resistant to morpholino knockdown of *vegfd*, a Kdr-specific ligand. Together, our data suggest that Plxnd1 antagonises Kdr/Vegfr signalling to limit lymphatic growth.

While Plxnd1 is known to regulate primary angiogenic sprouting (Childs et al., 2002; Torres-Vázquez et al., 2004), we show that it also regulates secondary sprouting from the posterior cardinal vein. Interestingly, despite an increase in secondary sprouting, there was no change in the number of *prox1a*-expressing lymphatic progenitors within the PCV or in parachordal LEC formation in our *plxnd1*^{nz75} mutant fish. Instead, the extra secondary sprouts were biased towards a venous fate to match the earlier increase in primary sprouting from the DA. This resulted in a roughly twofold increase in the number of both aISVs and vISVs, and therefore the ratio of aISVs to vISVs was unchanged in *plxnd1*^{nz75} mutants. This observation supports previous studies showing that the balance between arterial and venous ISVs is tightly regulated (Bussmann et al., 2010; Geudens et al., 2019, 2010).

It has been shown that the arteriovenous fate of ISVs is determined by the levels of Notch signalling in the primary ISVs and by an adaptive flow-mediated mechanism that together ensure a 1:1 ratio of arteries to veins (Geudens et al., 2019). Therefore, the fate of each secondary sprout is largely determined by the fate of the ISV that it engages with. While Prox1a signalling is required for lymphatic specification (Koltowska et al., 2015; Nicenboim et al., 2015), live imaging has revealed that lymphatic progenitors can arise from secondary sprouts that form no stable connection with an ISV (non-venous) but also from secondary sprouts that connect to an ISV and become venous (Geudens et al., 2019; Isogai et al., 2003). Together, these data support the idea that the mechanisms that promote the formation of secondary sprouts are distinct from the mechanisms involved in determining their fate. Our data suggest that while *plxnd1* normally inhibits secondary sprouting, likely by antagonising the Vegfr3/Erk pathway, *plxnd1* does not regulate arterial-venous fate decisions or the induction of *Prox1a* and lymphatic fate.

We have shown that Plxnd1 is an important regulator of developing lymphatics in zebrafish. The severity of the misguidance phenotype in *plxnd1* mutants suggests that Sema3/Plxnd1 signalling plays a major role in shaping the anatomy of the lymphatic network. We have also identified a role for *plxnd1* as an inhibitor of lymphangiogenesis by antagonising Kdr/Vegfr signalling within fLECs. These data demonstrate that not only is lymphatic migration regulated by *plxnd1* but that, in certain contexts, it is also required to ensure the correct levels of lymphangiogenesis. Based on previously observed conservation of PLXND1 function, it is highly likely that it also acts as broad regulator of lymphatic growth in mammals (Liu et al., 2016; Maruyama et al., 2021; Yang et al., 2012). Dysregulated lymphatic development underpins a number of human health conditions; lymphatic overgrowth in tumours is associated with metastasis, while lack of lymphatic regeneration following lymph node removal promotes cancer-associated secondary lymphoedema (Gousopoulos et al., 2017; Saito et al., 2013; Yoon et al., 2003). Currently, the VEGFC/VEGFR3 pathway is the key target for regulating lymphatic development. Our data identify the PLXND1 pathway as a potential additional therapeutic target in the treatment of lymphatic pathologies. The use of antibodies, shRNA, injection of ligands or cell-permeable peptides that target the cytosolic domain of PLXND1 could be used to inhibit or stimulate PLXND1 signalling in order to therapeutically promote or suppress lymphangiogenesis (Dieterich and Detmar, 2015; Fukushima et al., 2011; Moriya et al., 2010; Stacker et al., 2014; Vivekanandhan et al., 2021; Zhou et al., 2018). Importantly, therapeutically targeting PLXND1 can likely synergise with existing strategies targeting the VEGFC/VEGFR3 pathway and allow additional therapeutic control of lymphatic growth.

MATERIALS AND METHODS

Zebrafish lines and husbandry

All zebrafish strains were maintained under standard husbandry conditions. The lines used in this study were: wild type (AB), *plxnd1*^{fov01b} (Childs et al., 2002), *sema3aa*^{sa10241} and *sema3c*^{sa15161} (Kettleborough et al., 2013), *Tg(lyve1b:EGFP)*^{nz150}, *Tg(lyve1b:DsRed)*^{nz101} (Okuda et al., 2012), *Tg(fli1a:EGFP)*^{y1} (Lawson and Weinstein, 2002), *Tg(fli1a:nlsEGFP)*^{y7} (Roman et al., 2002), *Tg(kdrl:EGFP)*^{s843} (Jin et al., 2005), *Tg(kdrl:nlsmCherry)*^{nz49} (Lam et al., 2010), *Tg(kdrl:RFP)*^{la4} (Huang et al., 2005) and *Tg(prox1a:KalTA4)*^{uq3bh}; *Tg(10xUAS: Venus)* (known as *prox1a:Venus*; Koltowska et al., 2015). *plxnd1*^{nz75} was generated in this study.

ENU mutagenesis

ENU mutagenesis was performed as previously described (Solnica-Krezel et al., 1994). Briefly, *Tg(lyve1:DsRed)*^{nz101} males were mutagenised with weekly 1 h exposures to 3 mM ENU (Sigma) over 5 weeks and crossed with wild-type *lyve1:DsRed* females to produce F1 families. Subsequent incrossing of F2 progeny generated F3 embryos that were screened for misguided lymphatics.

Identification of the *nz75* mutant by positional cloning

Genomic DNA from pooled *nz75* mutant larvae and wild-type siblings (48 larvae each) was isolated using DNeasy Blood+Tissue kits (Qiagen) and converted into libraries using the SureSelect^{XT} library preparation kit (Agilent Technologies) according to the manufacturer's instructions. Sequencing of libraries was performed on an Illumina NextSeq 500 with 150 bp paired-end reads. We obtained ∼65 million reads per library.

The *nz75* mutation was then mapped using the raw fastq files with the SNPtrack algorithm (http://genetics.bwh.harvard.edu/snptrack/#), which maps the mutation to a genomic region by calculating the homozygosity score, expressed as a ratio of heterozygous SNP calls between wild-type and mutant pools multiplied by the number of informative homozygous SNP calls in the mutant pool (Leshchiner et al., 2012).

RNA was extracted from both *plxnd1*^{nz75} mutant and wild-type siblings, and cDNA was generated using random hexamer primers. Eight overlapping PCR products (see Table S1 for primer sequences) within the coding region of *plxnd1* were generated, sequenced and aligned to the reference to identify the *nz75* mutation.

Genotyping semaphorin mutants

sema3aa^{sa10241} and *sema3*^{sa15161} mutants were genotyped through the Sanger sequencing of genomic PCR products from whole larvae after imaging at 6 dpf (see Table S1 for primer sequences).

Whole mount *in situ* hybridisation

In situ hybridisation for *plxnd1*, *egfp, sema3ab* and *sema3c* were performed on whole zebrafish larvae using the *in situ* HCR kit (Molecular Instruments) according to manufacturer's instructions (Choi et al., 2018). *In situ* hybridisation for *sema3aa* was performed as described previously (Jowett and Lettice, 1994) using a 717 bp antisense, digoxigenin-labelled (DIG-labelled) riboprobe (see Table S1 for primer sequences used).

Development (2022) 149, dev200560. doi:10.1242/dev.200560

Morpholino injections

Morpholino injections were conducted as previously described (Nasevicius and Ekker, 2000). Morpholino sequences and doses are given in Table S2. The *plxnd1* (Torres-Vázquez et al., 2004) and *vegfd* MOs (Astin et al., 2014a; Bower et al., 2017) have been previously validated by comparison with a corresponding null mutant allele as per field guidelines (Stainier et al., 2017).

Inhibitor treatments

The embryos were raised to 2 dpf (in order to assess the effect on the misguidance phenotype) or 3 dpf (in order to assess the effect on the overgrowth phenotype), and then placed in a solution of 0.5% DMSO, 2 nM tivozanib (Aveo Pharmaceuticals), 1 µM sunitinib (Sigma-Aldrich) or 5 µM SL327 (Abcam), and the larvae were maintained in this solution until 6 dpf.

Cell transplantation

Cell transplantation was performed on 3 hpf embryos after manually dechorionating them on an agar bed. *lyve1b:DsRed; kdrl:EGFP* donor and *fli1a:EGFP* recipient embryos were placed into the troughs of an agar bed that was made using a transplantation mould (Adaptive Science Tools). Cells in the donor embryo were removed from ∼1/10th of the distance from the yolk sac to the animal pole using a borosilicate microinjection needle attached to an Eppendorf CellTram, and then 10-20 cells were transplanted into the same region of the blastula on the recipient embryo. Transplanted recipients were collected and maintained in E3 solution on an agar bed until 24 hpf, after which they were raised according to standard husbandry conditions. Successful grafts were identified by *lyve1:DsRed* expression and were imaged at 6 dpf.

Immunohistochemistry

Immunohistochemistry to detect pErk within the PCV and the facial lymphatics was performed on *lyve1b:EGFP* embryos using chicken anti-EGFP (Abcam, ab13970, 1:500) and rabbit anti-p44/42 MAPK (Cell Signaling Technology, 4370, 1:250) antibodies as described previously (Okuda et al., 2018).

RT-PCR

Reverse transcription PCR (RT-PCR) was used to confirm the expression of semaphorin genes. Larvae at 22, 30 or 48 hpf had their head and trunk tissue removed by dissection with a scalpel and total RNA was extracted. cDNA synthesis was conducted using random hexamer primers on 2 µg of total RNA before PCR with gene-specific primers (see Table S1 for primer sequences used).

Confocal live imaging of zebrafish

Embryos were imaged as described previously (Eng and Astin, 2018) with a Nikon D-Eclipse C1 confocal microscope or with an Olympus FV1000 confocal microscope for time-lapse microscopy. Still images were taken using *z* stacks 5 µm apart. For time-lapse microscopy, *z* stacks 5 µm apart were taken at 15 min intervals. Confocal images in this study are maximum projections of *z* series stacks. Images were processed using ImageJ (NIH), Photoshop CS5 (Adobe) and Volocity 5.4 image analysis software (Improvision/PerkinElmer Life and Analytical Sciences).

Zebrafish image analysis and statistics

Thoracic duct formation was quantitated by live imaging *lyve1b:DsRed* larvae at 6 dpf and measuring the percentage of somites 7-17 containing a segment of TD (Astin et al., 2014a). Aberrant facial lymphatics were identified as any branches not typically seen in the OLV, MFL and LFL, as previously defined (Eng and Astin, 2018). Misaligned ISLVs were quantitated by live imaging *lyve1b:DsRed; kdrl:EGFP* or *lyve1b:DsRed; fli1a:EGFP* larvae at 6 dpf and counting any ISLVs that were not completely aligned with an ISV across somites 7-11. For grafted animals, quantitation was conducted in the regions containing donor cells, as identified by *lyve1:DsRed*-expressing cells. Facial LECs (Eng and Astin, 2018) and trunk LECs were quantitated as previously described (Okuda et al., 2018).

Aberrant ISVs were counted by live imaging *kdrl:EGFP* embryos at 48 hpf and identifying all the ISVs between somites 7 and 11 that could be seen just dorsal to the DA and then counting as aberrant those that did not arise from the DA at a position aligned with an intersomitic boundary. Artery:vein ratio was quantitated by live imaging *kdrl:EGFP* larvae at 3 dpf and identifying them as aISVs or vISVs based on their connection to the DA or PCV, respectively. Secondary sprouts were counted between somites 7-11 by live imaging *lyve1b:EGFP* embryos at 36 hpf. Parachordal LEC formation was quantitated by live imaging *lyve1b:EGFP* larvae at 48 hpf and measuring the percentage of somites 7-17 containing a LEC(s) (Astin et al., 2014b).

ISLV time-lapse analysis was conducted by time-lapse imaging *lyve1b:DsRed; kdrl:EGFP* larvae from 50-75 hpf and identifying an ISLV that grows from the horizontal myoseptum and subsequently displays 6 h of growth for analysis. The aISV contact percentage was calculated as the percentage of time that the ISLV was no more than 20 µm from an aISV. The meandering index was determined by dividing the total growth of the ISLV (including branches that later retracted) over the net migration distance and the number of branching events was counted for each ISLV to give branching events/hour.

Statistical analysis was performed using Prism 5.0 software (GraphPad). Normality of distribution of data was identified by Shapiro-Wilks test. Significance of two sets of data was determined by Mann–Whitney or *t*-tests depending on whether the data were normally distributed. Significance across three or more sets of data was determined by one-way ANOVA or Kruskal–Wallis tests, depending on whether the data were normally distributed. Welch's correction was performed if different variances were detected.

Acknowledgements

We thank Alhad Mahagaonkar for expert management of our zebrafish facility, and the Biomedical Imaging Research Unit (School of Medical Sciences, University of Auckland), Yang Deng, Michael Cammer and NYU School of Medicine's Microscopy Laboratory (NCRR S10 RR024708) for assistance in confocal microscopy.

Competing interests

The authors declare no competing or financial interests.

Author contributions

Conceptualization: K.E.C., P.S.C., S.K.B., B.M.H., C.J.H., J.T.-V., J.W.A.; Methodology: P.M.K., L.G., K.E.C., S.K.B., B.M.H., C.J.H., J.T.-V.; Formal analysis: P.M.K., S.K.B.; Investigation: D.D.B., J.H., J.P.M., W.C., P.M.K., C.D.H., J.W.A.; Resources: B.M.H.; Writing - original draft: K.E.C., P.S.C., S.K.B., B.M.H., C.J.H., J.T.-V., J.W.A.; Visualization: P.S.C., J.W.A.; Supervision: S.K.B., B.M.H., C.J.H., J.T.-V., J.W.A.; Project administration: J.W.A.; Funding acquisition: P.S.C., S.K.B., J.T.-V., J.W.A.

Funding

This work was supported by the Health Research Council of New Zealand (14/105 to J.W.A.), and by the Marsden Funds, awarded by the Royal Society of New Zealand (UOA1602 and 20-UOA-27 to J.W.A.). S.K.B. and P.M.K. were supported by the Family of Marijana Kumerich and by Leukaemia and Blood Cancer New Zealand. Grants 5R01HL133687 and 1R01HL161090-01A1 (to J.T.-V.) from the National Heart Lung and Blood Institute (NHLBI), National Institutes of Health (NIH, United States of America) supported the work by J.H. and J.T.-V. Deposited in PMC for release after 12 months.

Peer review history

The peer review history is available online at https://journals.biologists.com/dev/lookup/doi/10.1242/dev.200560.reviewer-comments.pdf.

References

Astin, J. W., Haggerty, M. J. L., Okuda, K. S., Le Guen, L., Misa, J. P., Tromp, A., Hogan, B. M., Crosier, K. E. and Crosier, P. S. (2014a). Vegfd can compensate for loss of Vegfc in zebrafish facial lymphatic sprouting. *Development* **141**, 2680-2690. doi:10.1242/dev.106591

Astin, J. W., Jamieson, S. M. F., Eng, T. C. Y., Flores, M. V., Misa, J. P., Chien, A., Crosier, K. E. and Crosier, P. S. (2014b). An in vivo antilymphatic screen in zebrafish identifies novel inhibitors of Mammalian lymphangiogenesis and lymphatic-mediated metastasis. *Mol. Cancer Ther.* **13**, 2450-2462. doi:10.1158/1535-7163.MCT-14-0469-T

Aurandt, J., Li, W. and Guan, K.-L. (2006). Semaphorin 4D activates the MAPK pathway downstream of plexin-B1. *Biochem. J.* **394**, 459-464. doi:10.1042/BJ20051123

Baek, S., Oh, T. G., Secker, G., Sutton, D. L., Okuda, K. S., Paterson, S., Bower, N. I., Toubia, J., Koltowska, K., Capon, S. J. et al. (2019). The alternative splicing regulator Nova2 constrains vascular Erk signaling to limit specification of the lymphatic lineage. *Dev. Cell* **49**, 279-292.e275. doi:10.1016/j.devcel.2019.03.017

Basile, J. R., Gavard, J. and Gutkind, J. S. (2007). Plexin-B1 utilizes RhoA and Rho kinase to promote the integrin-dependent activation of Akt and ERK and endothelial cell motility. *J. Biol. Chem.* **282**, 34888-34895. doi:10.1074/jbc.M705467200

Bower, N. I., Vogrin, A. J., Le Guen, L., Chen, H., Stacker, S. A., Achen, M. G. and Hogan, B. M. (2017). Vegfd modulates both angiogenesis and lymphangiogenesis during zebrafish embryonic development. *Development* **144**, 507-518. doi:10.1242/dev.146969

Bribián, A., Nocentini, S., Llorens, F., Gil, V., Mire, E., Reginensi, D., Yoshida, Y., Mann, F. and del Río, J. A. (2014). Sema3E/PlexinD1 regulates the migration of hem-derived Cajal-Retzius cells in developing cerebral cortex. *Nat. Commun.* **5**, 4265. doi:10.1038/ncomms5265

Brouillard, P., Witte, M. H., Erickson, R. P., Damstra, R. J., Becker, C., Quéré, I. and Vikkula, M. (2021). Primary lymphoedema. *Nat. Rev. Dis. Primers* **7**, 77. doi:10.1038/s41572-021-00309-7

Burk, K., Mire, E., Bellon, A., Hocine, M., Guillot, J., Moraes, F., Yoshida, Y., Simons, M., Chauvet, S. and Mann, F. (2017). Post-endocytic sorting of Plexin-D1 controls signal transduction and development of axonal and vascular circuits. *Nat. Commun.* **8**, 14508. doi:10.1038/ncomms14508

Bussmann, J., Bos, F. L., Urasaki, A., Kawakami, K., Duckers, H. J. and Schulte-Merker, S. (2010). Arteries provide essential guidance cues for lymphatic endothelial cells in the zebrafish trunk. *Development* **137**, 2653-2657. doi:10.1242/dev.048207

Callander, D. C., Lamont, R. E., Childs, S. J. and McFarlane, S. (2007). Expression of multiple class three semaphorins in the retina and along the path of zebrafish retinal axons. *Dev. Dyn.* **236**, 2918-2924. doi:10.1002/dvdy.21315

Carretero-Ortega, J., Chhangawala, Z., Hunt, S., Narvaez, C., Menendez-Gonzalez, J., Gay, C. M., Zygmunt, T., Li, X. and Torres-Vazquez, J. (2019). GIPC proteins negatively modulate Plexind1 signaling during vascular development. *eLife* **8**, e30454. doi:10.7554/eLife.30454

Cha, Y. R., Fujita, M., Butler, M., Isogai, S., Kochhan, E., Siekmann, A. F. and Weinstein, B. M. (2012). Chemokine signaling directs trunk lymphatic network formation along the preexisting blood vasculature. *Dev. Cell* **22**, 824-836. doi:10.1016/j.devcel.2012.01.011

Childs, S., Chen, J.-N., Garrity, D. M. and Fishman, M. C. (2002). Patterning of angiogenesis in the zebrafish embryo. *Development* **129**, 973-982. doi:10.1242/dev.129.4.973

Choi, Y. I., Duke-Cohan, J. S., Chen, W., Liu, B., Rossy, J., Tabarin, T., Ju, L., Gui, J., Gaus, K., Zhu, C. et al. (2014). Dynamic control of beta1 integrin adhesion by the plexinD1-sema3E axis. *Proc. Natl. Acad. Sci. USA* **111**, 379-384. doi:10.1073/pnas.1314209111

Choi, H. M. T., Schwarzkopf, M., Fornace, M. E., Acharya, A., Artavanis, G., Stegmaier, J., Cunha, A. and Pierce, N. A. (2018). Third-generation in situ hybridization chain reaction: multiplexed, quantitative, sensitive, versatile, robust. *Development* **145**, dev165753. doi:10.1242/dev.165753

Coso, S., Zeng, Y., Opeskin, K. and Williams, E. D. (2012). Vascular endothelial growth factor receptor-3 directly interacts with phosphatidylinositol 3-kinase to regulate lymphangiogenesis. *PLoS ONE* **7**, e39558. doi:10.1371/journal.pone.0039558

Dashkevich, A., Raissadati, A., Syrjälä, S. O., Zarkada, G., Keränen, M. A. I., Tuuminen, R., Krebs, R., Anisimov, A., Jeltsch, M., Leppänen, V.-M. et al. (2016). Ischemia-reperfusion injury enhances lymphatic endothelial VEGFR3 and rejection in cardiac allografts. *Am. J. Transplant.* **16**, 1160-1172. doi:10.1111/ajt.13564

Deng, Y., Zhang, X. and Simons, M. (2015). Molecular controls of lymphatic VEGFR3 signaling. *Arterioscler. Thromb. Vasc. Biol.* **35**, 421-429. doi:10.1161/ATVBAHA.114.304881

Dieterich, L. C. and Detmar, M. (2015). Tumor lymphangiogenesis and new drug development. *Adv. Drug Deliv. Rev.* **99**, 148-160. doi:10.1016/j.addr.2015.12.011

Dietrich, T., Bock, F., Yuen, D., Hos, D., Bachmann, B. O., Zahn, G., Wiegand, S., Chen, L. and Cursiefen, C. (2010). Cutting edge: lymphatic vessels, not blood vessels, primarily mediate immune rejections after transplantation. *J. Immunol.* **184**, 535-539. doi:10.4049/jimmunol.0903180

Driessens, M. H. E., Hu, H., Nobes, C. D., Self, A., Jordens, I., Goodman, C. S. and Hall, A. (2001). Plexin-B semaphorin receptors interact directly with active Rac and regulate the actin cytoskeleton by activating Rho. *Curr. Biol.* **11**, 339-344. doi:10.1016/S0960-9822(01)00092-6

Eng, T. C. Y. and Astin, J. W. (2018). Characterization of Zebrafish facial lymphatics. *Methods Mol. Biol.* **1846**, 71-83. doi:10.1007/978-1-4939-8712-2_5

Eng, T. C. Y., Chen, W., Okuda, K. S., Misa, J. P., Padberg, Y., Crosier, K. E., Crosier, P. S., Hall, C. J., Schulte-Merker, S., Hogan, B. M. et al. (2019). Zebrafish facial lymphatics develop through sequential addition of venous and non-venous progenitors. *EMBO Rep.* **20**, e47079. doi:10.15252/embr.201847079

Fukushima, Y., Okada, M., Kataoka, H., Hirashima, M., Yoshida, Y., Mann, F., Gomi, F., Nishida, K., Nishikawa, S.-I. and Uemura, A. (2011). Sema3E-PlexinD1 signaling selectively suppresses disoriented angiogenesis in ischemic retinopathy in mice. *J. Clin. Invest.* **121**, 1974-1985. doi:10.1172/JCI44900

Gay, C. M., Zygmunt, T. and Torres-Vázquez, J. (2011). Diverse functions for the semaphorin receptor PlexinD1 in development and disease. *Dev. Biol.* **349**, 1-19. doi:10.1016/j.ydbio.2010.09.008

Geudens, I., Herpers, R., Hermans, K., Segura, I., Ruiz de Almodovar, C., Bussmann, J., De Smet, F., Vandevelde, W., Hogan, B. M., Siekmann, A. et al. (2010). Role of delta-like-4/Notch in the formation and wiring of the lymphatic network in zebrafish. *Arterioscler. Thromb. Vasc. Biol.* **30**, 1695-1702. doi:10.1161/ATVBAHA.110.203034

Geudens, I., Coxam, B., Alt, S., Gebala, V., Vion, A.-C., Meier, K., Rosa, A. and Gerhardt, H. (2019). Artery-vein specification in the zebrafish trunk is pre-patterned by heterogeneous Notch activity and balanced by flow-mediated fine-tuning. *Development* **146**, dev181024. doi:10.1242/dev.181024

Gitler, A. D., Lu, M. M. and Epstein, J. A. (2004). PlexinD1 and semaphorin signaling are required in endothelial cells for cardiovascular development. *Dev. Cell* **7**, 107-116. doi:10.1016/j.devcel.2004.06.002

Gousopoulos, E., Proulx, S. T., Bachmann, S. B., Dieterich, L. C., Scholl, J., Karaman, S., Bianchi, R. and Detmar, M. (2017). An Important Role of VEGF-C in Promoting Lymphedema Development. *J. Invest. Dermatol.* **137**, 1995-2004. doi:10.1016/j.jid.2017.04.033

Grimm, L., Nakajima, H., Chaudhury, S., Bower, N. I., Okuda, K. S., Cox, A. G., Harvey, N. L., Koltowska, K., Mochizuki, N. and Hogan, B. M. (2019). Yap1 promotes sprouting and proliferation of lymphatic progenitors downstream of Vegfc in the zebrafish trunk. *eLife* **8**, e42881. doi:10.7554/eLife.42881

Gu, C., Yoshida, Y., Livet, J., Reimert, D. V., Mann, F., Merte, J., Henderson, C. E., Jessell, T. M., Kolodkin, A. L. and Ginty, D. D. (2005). Semaphorin 3E and plexin-D1 control vascular pattern independently of neuropilins. *Science* **307**, 265-268. doi:10.1126/science.1105416

Hägerling, R., Pollmann, C., Andreas, M., Schmidt, C., Nurmi, H., Adams, R. H., Alitalo, K., Andresen, V., Schulte-Merker, S. and Kiefer, F. (2013). A novel multistep mechanism for initial lymphangiogenesis in mouse embryos based on ultramicroscopy. *EMBO J.* **32**, 629-644. doi:10.1038/emboj.2012.340

Hamm, M. J., Kirchmaier, B. C. and Herzog, W. (2016). Sema3d controls collective endothelial cell migration by distinct mechanisms via Nrp1 and PlxnD1. *J. Cell Biol.* **215**, 415-430. doi:10.1083/jcb.201603100

Hogan, B. M., Bos, F. L., Bussmann, J., Witte, M., Chi, N. C., Duckers, H. J. and Schulte-Merker, S. (2009a). Ccbe1 is required for embryonic lymphangiogenesis and venous sprouting. *Nat. Genet.* **41**, 396-398. doi:10.1038/ng.321

Hogan, B. M., Herpers, R., Witte, M., Heloterä, H., Alitalo, K., Duckers, H. J. and Schulte-Merker, S. (2009b). Vegfc/Flt4 signalling is suppressed by Dll4 in developing zebrafish intersegmental arteries. *Development* **136**, 4001-4009. doi:10.1242/dev.039990

Huang, H., Zhang, B., Hartenstein, P. A., Chen, J. N. and Lin, S. (2005). NXT2 is required for embryonic heart development in zebrafish. *BMC Dev. Biol.* **5**, 7. doi:10.1186/1471-213X-5-7

Ishii, E., Shimizu, A., Kuwahara, N., Arai, T., Kataoka, M., Wakamatsu, K., Ishikawa, A., Nagasaka, S. and Fukuda, Y. (2010). Lymphangiogenesis associated with acute cellular rejection in rat liver transplantation. *Transplant. Proc.* **42**, 4282-4285. doi:10.1016/j.transproceed.2010.09.081

Isogai, S., Lawson, N. D., Torrealday, S., Horiguchi, M. and Weinstein, B. M. (2003). Angiogenic network formation in the developing vertebrate trunk. *Development* **130**, 5281-5290. doi:10.1242/dev.00733

Ito, T., Morita, T., Yoshida, K., Negishi, T. and Yukawa, K. (2014). Semaphorin 3A-Plexin-A1 signaling through ERK activation is crucial for Toll-like receptor-induced NO production in BV-2 microglial cells. *Int. J. Mol. Med.* **33**, 1635-1642. doi:10.3892/ijmm.2014.1727

Jin, S.-W., Beis, D., Mitchell, T., Chen, J.-N. and Stainier, D. Y. R. (2005). Cellular and molecular analyses of vascular tube and lumen formation in zebrafish. *Development* **132**, 5199-5209. doi:10.1242/dev.02087

Jowett, T. and Lettice, L. (1994). Whole-mount in situ hybridizations on zebrafish embryos using a mixture of digoxigenin- and fluorescein-labelled probes. *Trends Genet.* **10**, 73-74. doi:10.1016/0168-9525(94)90220-8

Jung, H. M., Castranova, D., Swift, M. R., Pham, V. N., Venero Galanternik, M., Isogai, S., Butler, M. G., Mulligan, T. S. and Weinstein, B. M. (2017). Development of the larval lymphatic system in zebrafish. *Development* **144**, 2070-2081. doi:10.1242/dev.145755

Karkkainen, M. J., Haiko, P., Sainio, K., Partanen, J., Taipale, J., Petrova, T. V., Jeltsch, M., Jackson, D. G., Talikka, M., Rauvala, H. et al. (2004). Vascular endothelial growth factor C is required for sprouting of the first lymphatic vessels from embryonic veins. *Nat. Immunol.* **5**, 74-80. doi:10.1038/ni1013

Kettleborough, R. N. W., Busch-Nentwich, E. M., Harvey, S. A., Dooley, C. M., de Bruijn, E., van Eeden, F., Sealy, I., White, R. J., Herd, C., Nijman, I. J. et al. (2013). A systematic genome-wide analysis of zebrafish protein-coding gene function. *Nature* **496**, 494-497. doi:10.1038/nature11992

Kim, J., Oh, W.-J., Gaiano, N., Yoshida, Y. and Gu, C. (2011). Semaphorin 3E-Plexin-D1 signaling regulates VEGF function in developmental angiogenesis via a feedback mechanism. *Genes Dev.* **25**, 1399-1411. doi:10.1101/gad.2042011

Koltowska, K., Lagendijk, A. K., Pichol-Thievend, C., Fischer, J. C., Francois, M., Ober, E. A., Yap, A. S. and Hogan, B. M. (2015). Vegfc regulates bipotential precursor division and prox1 expression to promote lymphatic identity in zebrafish. *Cell Rep* **13**, 1828-1841. doi:10.1016/j.celrep.2015.10.055

Krueger, J., Liu, D., Scholz, K., Zimmer, A., Shi, Y., Klein, C., Siekmann, A., Schulte-Merker, S., Cudmore, M., Ahmed, A. et al. (2011). Flt1 acts as a negative regulator of tip cell formation and branching morphogenesis in the zebrafish embryo. *Development* **138**, 2111-2120. doi:10.1242/dev.063933

Küchler, A. M., Gjini, E., Peterson-Maduro, J., Cancilla, B., Wolburg, H. and Schulte-Merker, S. (2006). Development of the zebrafish lymphatic system requires VEGFC signaling. *Curr. Biol.* **16**, 1244-1248. doi:10.1016/j.cub.2006.05.026

Lam, E. Y. N., Hall, C. J., Crosier, P. S., Crosier, K. E. and Flores, M. V. (2010). Live imaging of Runx1 expression in the dorsal aorta tracks the emergence of blood progenitors from endothelial cells. *Blood* **116**, 909-914. doi:10.1182/blood-2010-01-264382

Lawson, N. D. and Weinstein, B. M. (2002). In vivo imaging of embryonic vascular development using transgenic zebrafish. *Dev. Biol.* **248**, 307-318. doi:10.1006/dbio.2002.0711

Leshchiner, I., Alexa, K., Kelsey, P., Adzhubei, I., Austin-Tse, C. A., Cooney, J. D., Anderson, H., King, M. J., Stottmann, R. W., Garnaas, M. K. et al. (2012). Mutation mapping and identification by whole-genome sequencing. *Genome Res.* **22**, 1541-1548. doi:10.1101/gr.135541.111

Lim, A. H., Suli, A., Yaniv, K., Weinstein, B., Li, D. Y. and Chien, C.-B. (2011). Motoneurons are essential for vascular pathfinding. *Development* **138**, 3847-3857. doi:10.1242/dev.068403

Liu, X., Uemura, A., Fukushima, Y., Yoshida, Y. and Hirashima, M. (2016). Semaphorin 3G provides a repulsive guidance cue to lymphatic endothelial cells via Neuropilin-2/PlexinD1. *Cell Rep.* **17**, 2299-2311. doi:10.1016/j.celrep.2016.11.008

Maruyama, K., Naemura, K., Arima, Y., Uchijima, Y., Nagao, H., Yoshihara, K., Singh, M. K., Uemura, A., Matsuzaki, F., Yoshida, Y. et al. (2021). Semaphorin3E-PlexinD1 signaling in coronary artery and lymphatic vessel development with clinical implications in myocardial recovery. *iScience* **24**, 102305. doi:10.1016/j.isci.2021.102305

Moriya, J., Minamino, T., Tateno, K., Okada, S., Uemura, A., Shimizu, I., Yokoyama, M., Nojima, A., Okada, M., Koga, H. et al. (2010). Inhibition of semaphorin as a novel strategy for therapeutic angiogenesis. *Circ. Res.* **106**, 391-398. doi:10.1161/CIRCRESAHA.109.210815

Nasevicius, A. and Ekker, S. C. (2000). Effective targeted gene 'knockdown' in zebrafish. *Nat. Genet.* **26**, 216-220. doi:10.1038/79951

Nicenboim, J., Malkinson, G., Lupo, T., Asaf, L., Sela, Y., Mayseless, O., Gibbs-Bar, L., Senderovich, N., Hashimshony, T., Shin, M. et al. (2015). Lymphatic vessels arise from specialized angioblasts within a venous niche. *Nature* **522**, 56-61. doi:10.1038/nature14425

Okuda, K. S., Astin, J. W., Misa, J. P., Flores, M. V., Crosier, K. E. and Crosier, P. S. (2012). lyve1 expression reveals novel lymphatic vessels and new mechanisms for lymphatic vessel development in zebrafish. *Development* **139**, 2381-2391. doi:10.1242/dev.077701

Okuda, K. S., Misa, J. P., Oehlers, S. H., Hall, C. J., Ellett, F., Alasmari, S., Lieschke, G. J., Crosier, K. E., Crosier, P. S. and Astin, J. W. (2015). A zebrafish model of inflammatory lymphangiogenesis. *Biol. Open* **4**, 1270-1280. doi:10.1242/bio.013540

Okuda, K. S., Baek, S. and Hogan, B. M. (2018). Visualization and tools for analysis of zebrafish lymphatic development. *Methods Mol. Biol.* **1846**, 55-70. doi:10.1007/978-1-4939-8712-2_4

Pedersen, M. S., Müller, M., Rülicke, T., Leitner, N., Kain, R., Regele, H., Wang, S., Gröne, H.-J., Rong, S., Haller, H. et al. (2020). Lymphangiogenesis in a mouse model of renal transplant rejection extends life span of the recipients. *Kidney Int.* **97**, 89-94. doi:10.1016/j.kint.2019.07.027

Peng, D., Ando, K., Hussmann, M., Gloger, M., Skoczylas, R., Mochizuki, N., Betsholtz, C., Fukuhara, S., Schulte-Merker, S., Lawson, N. D. et al. (2022). Proper migration of lymphatic endothelial cells requires survival and guidance cues from arterial mural cells. *eLife* **11**, e74094. doi:10.7554/eLife.74094.sa2

Roman, B. L., Pham, V. N., Lawson, N. D., Kulik, M., Childs, S., Lekven, A. C., Garrity, D. M., Moon, R. T., Fishman, M. C., Lechleider, R. J. et al. (2002). Disruption of acvrl1 increases endothelial cell number in zebrafish cranial vessels. *Development* **129**, 3009-3019. doi:10.1242/dev.129.12.3009

Saito, Y., Nakagami, H., Kaneda, Y. and Morishita, R. (2013). Lymphedema and therapeutic lymphangiogenesis. *Biomed. Res. Int.* **2013**, 804675. doi:10.1155/2013/804675

Sakurai, A., Gavard, J., Annas-Linhares, Y., Basile, J. R., Amornphimoltham, P., Palmby, T. R., Yagi, H., Zhang, F., Randazzo, P. A., Li, X. et al. (2010). Semaphorin 3E initiates antiangiogenic signaling through plexin D1 by regulating Arf6 and R-Ras. *Mol. Cell. Biol.* **30**, 3086-3098. doi:10.1128/MCB.01652-09

Sakurai, A., Jian, X., Lee, C. J., Manavski, Y., Chavakis, E., Donaldson, J., Randazzo, P. A. and Gutkind, J. S. (2011). Phosphatidylinositol-4-phosphate 5-kinase and GEP100/Brag2 protein mediate antiangiogenic signaling by semaphorin 3E-plexin-D1 through Arf6 protein. *J. Biol. Chem.* **286**, 34335-34345. doi:10.1074/jbc.M111.259499

Salameh, A., Galvagni, F., Bardelli, M., Bussolino, F. and Oliviero, S. (2005). Direct recruitment of CRK and GRB2 to VEGFR-3 induces proliferation, migration, and survival of endothelial cells through the activation of ERK, AKT, and JNK pathways. *Blood* **106**, 3423-3431. doi:10.1182/blood-2005-04-1388

Shin, M., Male, I., Beane, T. J., Villefranc, J. A., Kok, F. O., Zhu, L. J. and Lawson, N. D. (2016). Vegfc acts through ERK to induce sprouting and differentiation of trunk lymphatic progenitors. *Development* **143**, 3785-3795. doi:10.1242/dev.137901

Solnica-Krezel, L., Schier, A. F. and Driever, W. (1994). Efficient recovery of ENU-induced mutations from the zebrafish germline. *Genetics* **136**, 1401-1420. doi:10.1093/genetics/136.4.1401

Srinivasan, R. S., Dillard, M. E., Lagutin, O. V., Lin, F.-J., Tsai, S., Tsai, M.-J., Samokhvalov, I. M. and Oliver, G. (2007). Lineage tracing demonstrates the venous origin of the mammalian lymphatic vasculature. *Genes Dev.* **21**, 2422-2432. doi:10.1101/gad.1588407

Stacker, S. A., Williams, S. P., Karnezis, T., Shayan, R., Fox, S. B. and Achen, M. G. (2014). Lymphangiogenesis and lymphatic vessel remodelling in cancer. *Nat. Rev. Cancer* **14**, 159-172. doi:10.1038/nrc3677

Stainier, D. Y. R., Raz, E., Lawson, N. D., Ekker, S. C., Burdine, R. D., Eisen, J. S., Ingham, P. W., Schulte-Merker, S., Yelon, D., Weinstein, B. M. et al. (2017). Guidelines for morpholino use in zebrafish. *PLoS Genet.* **13**, e1007000. doi:10.1371/journal.pgen.1007000

Tanaka, H., Maeda, R., Shoji, W., Wada, H., Masai, I., Shiraki, T., Kobayashi, M., Nakayama, R. and Okamoto, H. (2007). Novel mutations affecting axon guidance in zebrafish and a role for plexin signalling in the guidance of trigeminal and facial nerve axons. *Development* **134**, 3259-3269. doi:10.1242/dev.004267

Tata, A., Stoppel, D. C., Hong, S., Ben-Zvi, A., Xie, T. and Gu, C. (2014). An image-based RNAi screen identifies SH3BP1 as a key effector of Semaphorin 3E-PlexinD1 signaling. *J. Cell Biol.* **205**, 573-590. doi:10.1083/jcb.201309004

Torres-Vázquez, J., Gitler, A. D., Fraser, S. D., Berk, J. D., Van, N. P., Fishman, M. C., Childs, S., Epstein, J. A. and Weinstein, B. M. (2004). Semaphorin-plexin signaling guides patterning of the developing vasculature. *Dev. Cell* **7**, 117-123. doi:10.1016/j.devcel.2004.06.008

Toyofuku, T., Yabuki, M., Kamei, J., Kamei, M., Makino, N., Kumanogoh, A. and Hori, M. (2007). Semaphorin-4A, an activator for T-cell-mediated immunity, suppresses angiogenesis via Plexin-D1. *EMBO J.* **26**, 1373-1384. doi:10.1038/sj.emboj.7601589

Uesugi, K., Oinuma, I., Katoh, H. and Negishi, M. (2009). Different requirement for Rnd GTPases of R-Ras GAP activity of Plexin-C1 and Plexin-D1. *J. Biol. Chem.* **284**, 6743-6751. doi:10.1074/jbc.M805213200

Vivekanandhan, S., Madamsetty, V. S., Angom, R. S., Dutta, S. K., Wang, E., Caulfield, T., Pletnev, A. A., Upstill-Goddard, R., Asmann, Y. W., Chang, D. et al. (2021). Role of PLEXIND1/TGFbeta signaling axis in pancreatic ductal adenocarcinoma progression correlates with the mutational status of KRAS. *Cancers (Basel)* **13**, 4048. doi:10.3390/cancers13164048

Vogrin, A. J., Bower, N. I., Gunzburg, M. J., Roufail, S., Okuda, K. S., Paterson, S., Headey, S. J., Stacker, S. A., Hogan, B. M. and Achen, M. G. (2019). Evolutionary differences in the Vegf/Vegfr code reveal organotypic roles for the endothelial cell receptor Kdr in developmental lymphangiogenesis. *Cell Rep.* **28**, 2023-2036.e2024. doi:10.1016/j.celrep.2019.07.055

Wang, Y., He, H., Srivastava, N., Vikarunnessa, S., Chen, Y.-B., Jiang, J., Cowan, C. W. and Zhang, X. (2012). Plexins are GTPase-activating proteins for Rap and are activated by induced dimerization. *Sci. Signal.* **5**, ra6. doi:10.1126/scisignal.2002636

Wang, G., Muhl, L., Padberg, Y., Dupont, L., Peterson-Maduro, J., Stehling, M., le Noble, F., Colige, A., Betsholtz, C., Schulte-Merker, S. et al. (2020). Specific fibroblast subpopulations and neuronal structures provide local sources of Vegfc-processing components during zebrafish lymphangiogenesis. *Nat. Commun.* **11**, 2724. doi:10.1038/s41467-020-16552-7

Wigle, J. T. and Oliver, G. (1999). Prox1 function is required for the development of the murine lymphatic system. *Cell* **98**, 769-778. doi:10.1016/S0092-8674(00)81511-1

Wigle, J. T., Harvey, N., Detmar, M., Lagutina, I., Grosveld, G., Gunn, M. D., Jackson, D. G. and Oliver, G. (2002). An essential role for Prox1 in the induction of the lymphatic endothelial cell phenotype. *EMBO J.* **21**, 1505-1513. doi:10.1093/emboj/21.7.1505

Wild, R., Klems, A., Takamiya, M., Hayashi, Y., Strähle, U., Ando, K., Mochizuki, N., van Impel, A., Schulte-Merker, S., Krueger, J. et al. (2017). Neuronal sFlt1 and Vegfaa determine venous sprouting and spinal cord vascularization. *Nat. Commun.* **8**, 13991. doi:10.1038/ncomms13991

Wong, B. W. (2020). Lymphatic vessels in solid organ transplantation and immunobiology. *Am. J. Transplant.* **20**, 1992-2000. doi:10.1111/ajt.15806

Wortzel, I. and Seger, R. (2011). The ERK cascade: distinct functions within various subcellular organelles. *Genes Cancer* **2**, 195-209. doi:10.1177/1947601911407328

Yang, Y., García-Verdugo, J. M., Soriano-Navarro, M., Srinivasan, R. S., Scallan, J. P., Singh, M. K., Epstein, J. A. and Oliver, G. (2012). Lymphatic endothelial progenitors bud from the cardinal vein and intersomitic vessels in mammalian embryos. *Blood* **120**, 2340-2348. doi:10.1182/blood-2012-05-428607

Yang, W.-J., Hu, J., Uemura, A., Tetzlaff, F., Augustin, H. G. and Fischer, A. (2015). Semaphorin-3C signals through Neuropilin-1 and PlexinD1 receptors to inhibit pathological angiogenesis. *EMBO Mol. Med.* **7**, 1267-1284. doi:10.15252/emmm.201404922

Yaniv, K., Isogai, S., Castranova, D., Dye, L., Hitomi, J. and Weinstein, B. M. (2006). Live imaging of lymphatic development in the zebrafish. *Nat. Med.* **12**, 711-716. doi:10.1038/nm1427

Yoon, Y.-S., Murayama, T., Gravereaux, E., Tkebuchava, T., Silver, M., Curry, C., Wecker, A., Kirchmair, R., Hu, C. S., Kearney, M. et al. (2003). VEGF-C gene therapy augments postnatal lymphangiogenesis and ameliorates secondary lymphedema. *J. Clin. Invest.* **111**, 717-725. doi:10.1172/JCI15830

Yu, H.-H. and Moens, C. B. (2005). Semaphorin signaling guides cranial neural crest cell migration in zebrafish. *Dev. Biol.* **280**, 373-385. doi:10.1016/j.ydbio.2005.01.029

Zhang, Y., Singh, M. K., Degenhardt, K. R., Lu, M. M., Bennett, J., Yoshida, Y. and Epstein, J. A. (2009). Tie2Cre-mediated inactivation of plexinD1 results in congenital heart, vascular and skeletal defects. *Dev. Biol.* **325**, 82-93. doi:10.1016/j.ydbio.2008.09.031

Zhang, Y. F., Zhang, Y., Jia, D. D., Yang, H. Y., Cheng, M. D., Zhu, W. X., Xin, H., Li, P. F. and Zhang, Y. F. (2021). Insights into the regulatory role of Plexin D1 signalling in cardiovascular development and diseases. *J. Cell. Mol. Med.* **25**, 4183-4194. doi:10.1111/jcmm.16509

Zhou, Y.-F., Li, P.-C., Wu, J.-H., Haslam, J. A., Mao, L., Xia, Y.-P., He, Q.-W., Wang, X.-X., Lei, H., Lan, X.-L. et al. (2018). Sema3E/PlexinD1 inhibition is a therapeutic strategy for improving cerebral perfusion and restoring functional loss after stroke in aged rats. *Neurobiol. Aging* **70**, 102-116. doi:10.1016/j.neurobiolaging.2018.06.003

Zygmunt, T., Gay, C. M., Blondelle, J., Singh, M. K., Flaherty, K. M. C., Means, P. C., Herwig, L., Krudewig, A., Belting, H.-G., Affolter, M. et al. (2011). Semaphorin-PlexinD1 signaling limits angiogenic potential via the VEGF decoy receptor sFlt1. *Dev. Cell* **21**, 301-314. doi:10.1016/j.devcel.2011.06.033